Applied Catalysis B: Environmental 254 (2019) 510–522

Contents lists available at ScienceDirect

Applied Catalysis B: Environmental

journal homepage: www.elsevier.com/locate/apcatb

Transition metal carbide catalysts for biomass conversion: A review

Jifeng Pang[a,b], Junming Sun[a,*], Mingyuan Zheng[b], Houqian Li[a], Yong Wang[a,c,**], Tao Zhang[b,*]

[a] The Gene and Linda Voiland School of Chemical Engineering and Bioengineering, Washington State University, Pullman, WA, 99164, USA
[b] Dalian Institute of Chemical Physics, Chinese Academy of Sciences, Dalian, 116023, PR China
[c] Institute for Integrated Catalysis and Environmental Molecular Sciences Laboratory, Pacific Northwest National Laboratory, Post Office Box 999, Richland, WA, 99352, USA

ARTICLE INFO

Keywords:
Transition metal carbide
Catalysis
Biomass
Glycols
Lignin
Hydrodexoygenation

ABSTRACT

The increasing demand for sustainable energy resources has initiated the investigation of biomass conversion over a wide range of catalysts. Among those, transition metal carbides have been extensively studied which demonstrated distinct reactivity and/or selectivity from transition or noble metals in a variety of chemical reactions. In this review, we summarize recent advances in the synthesis of transition metal carbides and their applications in biomass conversion, particularly focusing on the catalytic conversions of (hemi)cellulose, lignin and some typical platform chemicals to fuels or fine chemicals involving C—C, C—O—C and C—O—H bonds cleavages. Perspectives regarding the future research directions on the improvement of transition metal carbide catalysts and detailed reaction mechanism studies are also presented.

1. Introduction

The depletion of fossil resources and the incremental environmental regulations triggered the exploration of carbon neutral energy resources. Biomass is the only carbon containing renewable resource that could be readily integrated into the contemporary energy system [1,2]. Hence, the catalytically upgrading biomass to produce renewable chemicals and fuels has been extensively investigated [3–6].

Various types of catalysts have been applied in biomass conversion. Some oil refinery catalysts such as zeolites and hydrotreating catalysts have been used in the biorefinery process [7]. However, due to the high oxygen contents in biomass feedstocks and different reaction conditions, most of the petrochemical catalysts exhibited low activity and poor stability in biomass upgrading. Noble metals, on the other hand, are highly active and have been being widely studied in biomass conversion. Nevertheless, the limited availability of noble metals on earth has motivated the exploration of alternative catalysts which are inexpensive and and based on earth-abundant elements for biomass upgrading.

Since Levy and Boudart discovered the platinum-like properties of transition metal carbides, these noble metal-like catalysts have gained great attentions, and are considered as alternative inexpensive candidate catalysts, especially in the reactions involving hydrogen (e.g., hydrogenation) [8].

Transition metal carbides are interstitial alloys, which are prepared by incorporating carbon atoms into the lattices of transition metals, as shown in Fig. 1. The carbon atoms preferably occupy the largest sites available for parent metals, and the final structure of carbide is determined by geometric and electronic factors [9]. According to the geometric factor discovered by Hägg, only when the ratio of carbon to metal hard-ball radii is less than 0.59, the carbide structures shown in Fig. 1 can be formed. Meanwhile, the electronic factor can be interpreted by the Engel–Brewer theory of metals, which led to the formation of interstitial compounds via the interaction between the s–p orbitals of the carbon and the s–p–d band of the metal atoms [10,11]. The lattice carbon atom, in turn, lengthens the metal-metal bond distance, and thus changes the d-band electron density of metals at Fermi level via electron transfer from the metal atom to the carbon atom [12], causing the distinct adsorption/desorption properties with respect to its metal analogues [13,14]. Transition metal carbide has found wide applications in a variety of reactions such as ammonia synthesis and decomposition [15]. hydrazine decomposition [16], isomerization [17] and hydroprocessing [18]. Numerous researches and reviews have been dedicated to the application of carbides in hydrogen production, electro catalysts of fuel cells and the C1 based chemical conversions [19–26]. Owning to their unique properties, transition metal carbides have also been recently explored in biomass conversions, especially in the C—C, C–O-C and C–O-H bonds cleavage reactions [27–29]. In this review, we

* Corresponding author.
** Corresponding author at: The Gene and Linda Voiland School of Chemical Engineering and Bioengineering, Washington State University, Pullman, WA, 99164, USA.
E-mail addresses: junming.sun@wsu.edu (J. Sun), yong.wang@pnnl.gov (Y. Wang), taozhang@dicp.ac.cn (T. Zhang).

https://doi.org/10.1016/j.apcatb.2019.05.034
Received 6 March 2019; Received in revised form 5 May 2019; Accepted 8 May 2019
Available online 08 May 2019
0926-3373/

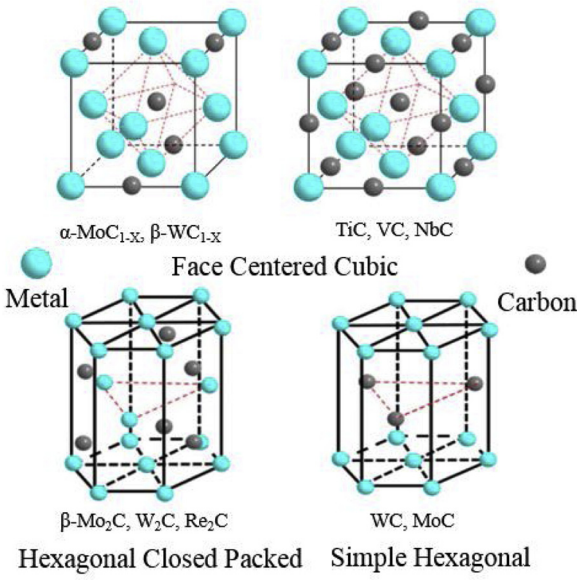

Fig. 1. Typical structures of transition metal carbide catalysts [23,30].

will focus on the advances of transition metal carbide catalysts in catalytic conversion of biomass, particularly in the areas of hydrotreating of lignocellulosic biomass and biomass derived platform chemicals. Specifically, the methodologies for metal carbide catalysts synthesis will be summarized. Then, the recent advances of metal carbide catalysts in (hemi) cellulose, lignin and some typical platform chemicals (i.e., fatty acid or ester, phenolics, furan based chemicals, acetic acid, levulinic acid) conversions will be discussed in detail. Finally, prospects regarding the future development of transition metal carbide catalysts will be given based on the state of the art synthesis and the applications of the carbide catalysts.

2. Methods for the synthesis of transition metal carbide catalysts

To prepare transition metal carbide catalysts, suitable carbon precursors including solid carbons, polymers, carbon containing chemicals, hydrocarbons, have been chosen. Based on the reaction phases by which the carbon precursors are involved in this synthesis, two methodologies are broadly categorized, i.e., solid-solid phase reaction (carbon source in solid form) and solid-gas phase reaction (carbon source in gas form).

2.1. Synthesis of transition metal carbide catalysts via the solid-solid phase reaction

As above-mentioned, the solid-solid phase reaction uses solid carbon materials as the carbon resource to incorporate C atoms into the lattice of metals. In this particularly case, the carbon resource can be directly from a solid carbon material such as activated carbon (AC) or carbon nanotubes (CNTs). More promisingly, carbon containing chemicals in liquid form could be used as a precursor/reactant to uniformly mix/react with the metal precursor, which results in a composite material with tailorable morph-structures and thus controlled structures/particles of metal carbide. These will be detailed in the following part of this section.

Initially, powder metallurgy method was used to synthesize the carbide catalysts, in which the metal oxide powders were carburized in the presence of solid carbon at a temperature as high as 1800 K [9]. Typically, the catalysts prepared by this method showed a very low surface area (< 10 m^2/g) and poor activity. A carbothermal method was then developed, where solid carbon reacted with vaporized metal oxides at temperatures higher than 1000 K to produce metal carbide catalysts. The surface area of the obtained carbides is slightly higher (20-40 m^2/g) than those prepared by the powder metallurgy method [9,31]. Later, researchers also developed a modified carbothermal method (i.e., carbothermal hydrogen reduction method) to prepare highly dispersed supported metal carbide catalysts at lower temperatures using a reducing agent. In this particular case, metal precursors were first deposited on a carbon support, which was then carburized under reducing atmosphere. The surface area of the transition metal carbide catalysts by this method could reach up to 200 m^2/g [32,33].

Following this promising reduction methodology, various strategies have been used to further improve the dispersion of transition metal carbides [34,35]. As the results, carbon support was found to affect the dispersion of the obtained carbide catalysts. For example, by employing an ultrahigh surface area carbon material (> 3000 m^2/g) as the carbon source and support, Liang et al. successfully synthesized a β-Mo_2C/AC catalyst with uniform particle size of 10 nm after carbothermal reduction in hydrogen at 973 K [36]. Similarly, Zhang et al. loaded ammonium metatungstate on the mesoporous carbon (MC), and carburized in a H_2 flow at 1173 K. The resulted WC_x nanoparticles were highly dispersed on the MC support with particle size being less than 10 nm [37]. Han et al. used CNTs as the support to prepare 20%Mo_2C/CNTs catalysts by the carbothermal hydrogen reduction method, and the particle size of the obtained Mo_2C (hcp) is 10.5 nm [38]. Besides the carbon support, the carbide precursor was also found crucial to the final carbides. Garcia-Esparza used the more active tungsten precursor (WCl_6) for tungsten carbides synthesis [39]. The WCl_6 was found to react with ethanol first, forming a stable intermediate of $WCl_3(OC_2H_5)_2$. The intermediate was then gradually transformed into W_2C/WC at the expense of mesoporous graphitic C_3N_4 at elevated temperatures (1073–1373 K). The particle size of the obtained carbide (W_2C or WC) is ca. 5 nm, which is much smaller than that derived from the ammonium metatungstate over active carbon supports (10–50 nm) [37]. In addition, the compositions and structures of the nano-carbide was found to be tunable depending on the composition of precursors and the reduction temperatures.

Based on the improved carbothermal reduction method, various carbides were synthesized over carbon supports [40,41]. Nevertheless, this method has the drawbacks of limited support choices, small metal-carbon interface, as well as formation of mixed carbide phases and difficulty in controlling the particle sizes. Therefore, various liquid carbon containing precursors were used to better control the structure and metal-carbon interface for the solid-solid phase reaction during the carbides synthesis. Hereinafter, this modified methodology is also named as liquid derived solid-solid process.

In particular, appropriate metal and carbon precursors are dissolved or mixed in liquid phase, where they react to form polymeric networks. The resulted solid is then carburized to form metal carbides in inert or reducing atmosphere. The typical liquid derived solid-solid processes to prepare metal carbides include the urea-glass and amine-oxide methods, as shown in Fig. 2. The urea-glass method was first developed by Giordano et al. to prepare both metal nitrides and carbides. For the carbide synthesis, urea is typically used as both the carbon-source and polymerizing agent. One example is that, $MoCl_5$ or WCl_4 first reacted with alcohols and urea to form a polymer-like material, which was then reduced to nitrides or carbides by simply varying the metal precursor/urea molar ratio [42,43]. Following this methodology, Liu et al. synthesized hexagonal α-Mo_2C catalysts for CO_2 conversion, and got the high selectivity towards CO [44]. For the amine-oxide method, amine is used as the carbon precursor for the synthesis of carbide catalysts as reported by Wan et al. [45]. Specifically, the ammonium molybdate and amines were mixed to form a solution, and then amine-metal oxide was precipitated out by adjusting the pH of the solution. After the carburization process at elevated temperatures, transition metal carbides were obtained. This method greatly decreased the diameter of final carbide particles (< 10 nm). It was also found that the morphologies and crystal structures of molybdenum carbides can be controlled by changing the

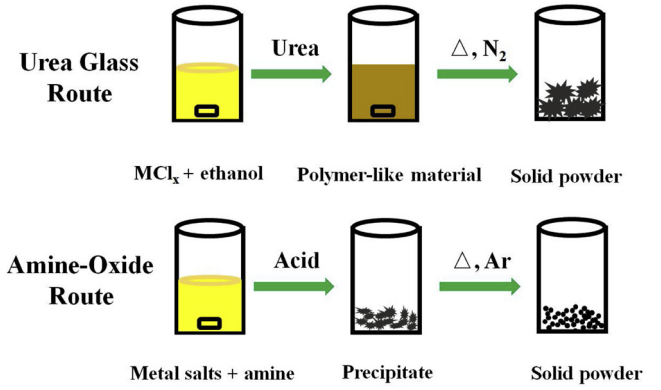

Fig. 2. Schematic representation of the urea-glass and amine-oxide routes [42,45].

amount of amines and carburized temperatures. Following this similar synthesis strategy, Wang et al. introduced the molybdenum precursor into the phenolic resin via a one-pot organic–organic cooperative self-assembly approach. After the carburization process, highly dispersed molybdenum carbide with particle size of 3–5 nm was fabricated in the ordered mesoporous carbon walls [46]. However, the produced carbide particles are prone to aggregate, and resulted in the fused bulk particles under high temperatures [47]. Differently, Gu et al. reported a sodium co-reduction of $MoCl_5$ and carbon tetrabromide in benzene to produce carbide catalysts. Although a lower reaction temperature was used (i.e., 623 K), the particles size of the Mo_2C still reached up to 30 nm [48].

To further improve the dispersion and stability of supported metal carbide catalysts, different bottom-up methods were explored using the liquid derived solid-solid phase reaction. The most promising one is to physically confine the carbide particles in a specific micro-environment, and prevent the particles from agglomeration. Baddour et al. used surface-modified mesoporous SBA-15 to load the ethanolic solution of $MoCl_5$ and 4-chloro-ortho-phenylenediamine. Owing to the hydrophobic of the produced Mo-4 chloro-ortho-phenylenediamine, the precursor prefers to stay within the modified mesopores during the synthesis, resulting in the formation of the confined molybdenum carbide nanoparticles [49]. The particle size of the produced α-MoC_{1-x} was only 1.9 nm, much smaller than the previous reports (ca. 5 nm). Han et al. reported the synthesis of carbon matrix confined WCx by a two-step process [50]. They first synthesized the tungsten–polydopamine hybrids using dopamine and metatungstate precursor and *in situ* polymerization. The tungsten species in the hybrid materials were located in the polymerized matrix, which eventually led to the formation of confined tungsten carbide (< 5 nm) after the carburization process. Xu et al. used a cage-confinement pyrolysis strategy to synthesis ultrasmall tungsten carbide nanoparticles [51]. As shown in Fig. 3, the authors used the zeolitic metal-azolate frameworks (MAFs) as a nano-reactor to confine $W(CO)_6$. During the carburization process, the carbon nano-polyhedron was maintained with the evaporation of zinc, and the carbides eventually formed in the carbon cage. Even at 1173 K, uniform WC nanoparticles with average sizes of 2 nm were successfully prepared. Similarly, Wan et al. synthesized 1D or 2D Mo_2C through carburized the cobalt or zinc-based metal-organic framework (ZIF-67 or ZIF-8) with confined MoO_3 nanosheets or nanowires (Fig. 3). The resulted carbides have large numbers of active sites for hydrogen evolution [52].

Other researchers also used the template method to restrict the particle size or the position of carbides. Yu et al. used the carboxylic polystyrene spheres as the hard template to load Mo species of bis (acetylacetonato)dioxomolybdenum(VI) in the presence of glucose and phenol [53]. After a calcination in flowing Ar/H_2 at 973–1073 K, the composite was successfully transformed into 3D ordered porous molybdenum carbides. The self-assembly method was also proved to be an efficient method for the transition metal carbide synthesis. For instance, Zhu et al. used a simple salt template method to prepare the metal carbide catalysts. They used 1-ethyl-3-methylimidazolium dicyanamide as the carbon resource, a mixture of KCl and $ZnCl_2$ as the salt template, and metal chlorides ($MoCl_6$, WCl_5, $TaCl_5$ or $NbCl_5$) as the metal precursor for this synthesis. After carburization and removal of the salt templates, the authors obtained different metal carbide nanoparticles (MoC, WC, TaC, NbC) with an average particle size of 3 nm, which were rigidly embedded into the vertically aligned two dimensional carbon nanosheets [54]. Chen et al. designed a three-dimensional hierarchical porous α-MoC_{1-x} catalyst via the self-polymerization of dopamine together with Mo salts. As shown in Fig. 4, dopamine molecules are spontaneous polymerized with $Mo_7O_{24}^{6-}$ anions, resulting in the formation of a Mo/polydopamine hybrid material with unique micro-flower morphology. Upon the carburization, Mo/polydopamine hybrid was converted into molybdenum carbides with the morphology being maintained [55].

In the past decade, the liquid derived solid-solid phase process has been rapidly developed due to the relatively mature solution, sol-gel and polymer chemistry, providing a versatile method for novel transition metal carbide synthesis.

2.2. Synthesis of transition metal carbide catalysts via the solid-gas phase reaction

The solid-gas phase reaction process is, so far, the prevailing way for carbide catalysts preparation. Generally, the metal salt loaded on supports was carburized in flowing CO, hydrocarbons gases (HC: CH_4, C_2H_6, C_3H_8, C_4H_{10} and aromatic compounds) with/without co-fed hydrogen. In 1980s, Boudart's group first reported this method for carbide synthesis, and named it as the temperature-programmed reduction method. In a typical process, the metal precursor was loaded on a support by impregnation or wet chemical methods. After the dry and/or calcination processes, the precursor was carburized in 20% CH_4/H_2 using the CH_4 as the carbon source. To obtain fine carbide particles, temperature programed carburization process was noted depending on the forms of metal and carbon precursors [9]. Additionally, the same group investigated the influence of preparation parameters on the final carbide properties. They found that the phase of transition metal carbides could be controlled by adjusting the carburation atmospheres. As shown in Fig. 5, orthorhombic MoO_3 with surface area less than 1 m^2/g is transformed into Mo_2C with surface area of 50-100 m^2/g upon carburization in CH_4/H_2 flow, but it changes to α-MoC_{1-x} with elevated surface area of 200 m^2/g after doped with 0.25%Pt. The same face-centered cubic α-MoC_{1-x} can also be obtained by temperature-programmed carburization of nitride that derived from the reaction of oxides with ammonia [56,57]. Similarly, three types of tungsten carbide could also be obtained by adjusting the carburization temperatures and atmospheres [58].

Since then, temperature-programmed reduction method has been widely used to prepare high surface area supported transition metal carbide catalysts including but not limited to non-carbon supports. Moreover, various methods have been developed to control the particle size and phases, as well as to stabilize the particles under reaction conditions. Hunt et al. used a three-step process to prepare uniform distributed metal carbide catalysts. As shown in Fig. 6, they first prepared the silica encapsulated transition-metal oxide via a reverse microemulsion method. The silica encapsulated metal oxide was then carburized under the CH_4/H_2 atmosphere. After removing the silica, the naked tungsten carbides were re-dispersed onto other supports. This method is a versatile technique to synthesize carbides in the 1–4 nm range with tunable size, composition, and crystal phase [59]. With the similar method, Jia et al. carburized Cu-MoO_2 rods in methane to get the Cu-Mo_2C particles over hierarchical porous carbon rods. After removing the Cu with $FeCl_3$ solutions, highly active Mo_2C on cross-linked porous carbon was obtained. It is also found that the Cu species were

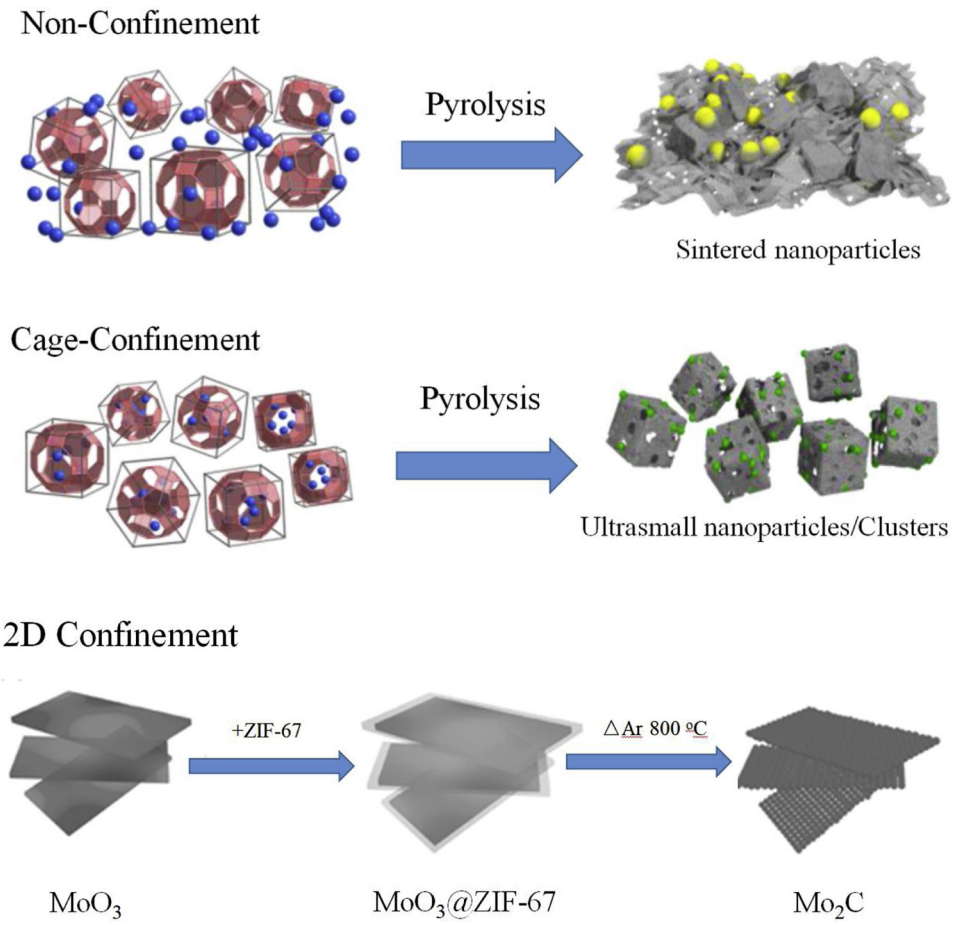

Fig. 3. Comparison of the non-confinement, cage and 2D confinement pyrolysis methods for transition metal carbides synthesis [51,52].

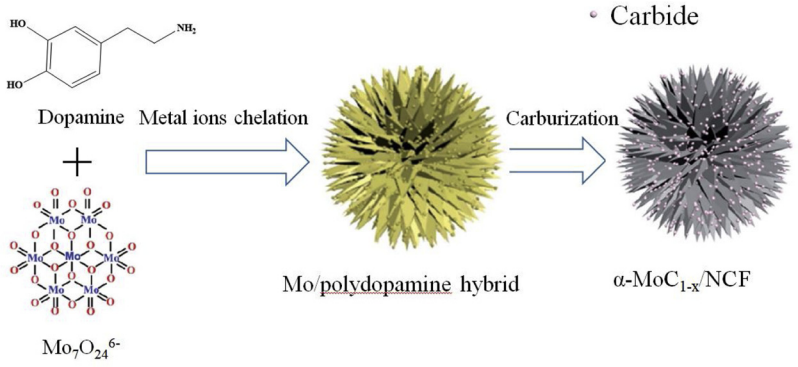

Fig. 4. The synthesis process of hierarchical α-MoC_{1-x}/NCF microflowers [55].

crucial to prepare the well separated Mo_2C particles, to generate the porous structure of carbon, and to protect the carbides from excess carbon coverage [60].

With the development of new technologies, other novel transition metal carbide synthesis methods have also been proposed. By using a plasma-assisted carburization method, Ren. et al. successfully converted the tungstic oxide to tungsten carbide hybrid with porous nanostructures and an appropriate carbon coating layer [61]. Other researchers also reported to use *in situ* ultra-high vacuum conditions to carburize Mo or W foil with ethylene, and produced phase-pure WC foils [62,63].

3. Catalytic conversion of biomass over transition metal carbide catalysts

Since the first report on the rearrangement of 1,1,3-trimethyl-cyclopentane to xylene [64], transition metal carbides have been extensively studied in isomerization, hydrodesulfurization, hydrodenitrogenation, electrocatalysts of fuel cells, and syngas conversion, which have been well discussed and summarized [65–67]. Other than those reactions, transition metal carbides have also been demonstrated as promising catalysts for biomass conversions [68–70]. In the following sections, the development of biomass conversion over transition metal carbides, i.e, catalytic conversion of (hemi)cellulose to glycols, selectively de-polymerization of lignin, and upgrading of some biochemicals to fine chemicals or fuels, will be detailed.

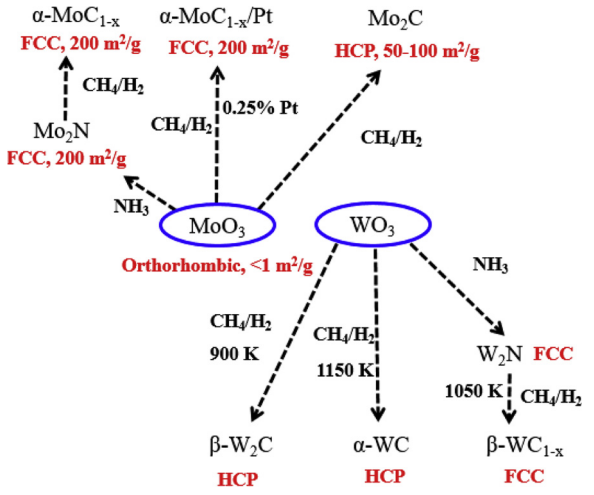

Fig. 5. Procedures for the synthesis of molybdenum and tungsten carbides (FCC: face centered cubic, HCP: hexagonal closed packed) [57,58].

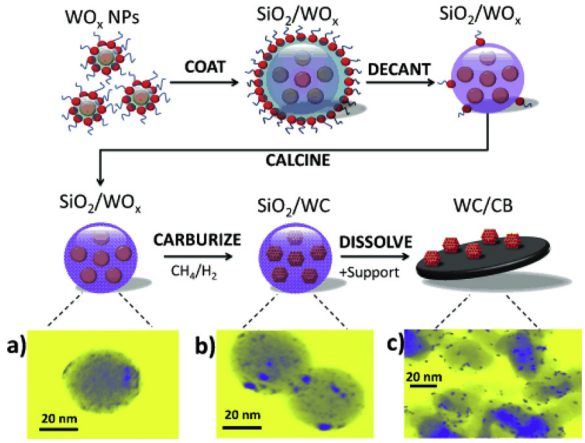

Fig. 6. Representation of the three-step process for the synthesis of WC/CB catalysts (CB: Vulcan XC-72 r carbon black) [59].

3.1. Catalytic conversion of (hemi) cellulose over transition metal carbides

Hemicellulose and cellulose are the major components in biomass, representing about 70% of plant cell. Hemicellulose is composed of heterogeneous polymers of pentoses (xylose, arabinose), hexoses (mannose, glucose, galactose), and some sugar acids [71]. In contrast, cellulose is a homogeneous polymer of cellobiose that linked by β-1,4-glycosidic bonds. It also has a highly crystallized structure and strong hydrogen bonds, which is resistant to being degraded under most conditions.

The products of cellulose conversion are highly dependent on the reaction conditions and catalysts. As shown in Fig. 7, mild reaction conditions with long reaction times are in favor of glucose production due to the metastable of produced sugars [72,73]. To improve the reaction efficiency, elevated temperatures and/or noble metal catalysts are required to produce more stable product, sorbitol, in hydrogen atmosphere [74–76]. Other than the extensive work on hydrocracking of hexitiols or glycerol to ethylene glycol (EG) over Ni, Cu or noble metal catalysts [77,78], an environmentally benign process for one-pot conversion of cellulose to EG was developed by Ji et al. [79]. Over the 2% Ni doped 30%W_2C/AC catalyst, the EG yield reached 61% at 100% cellulose conversion, which is much higher than those previously reported and comparison noble metal catalysts (ca. 5–30% vs 61%). The authors also tried different Mo_2C catalysts for this reaction. However, only 11% yield to EG was obtained at 87% cellulose conversion, and the tungsten based catalysts showed unique activity towards EG [80]. Different from sugars or sorbitol, EG is a petroleum-dependent monomer that has been widely used in polyester synthesis with an annual production of 26.4 million tons in 2016. The novel discovery opens a renewable way to convert biomass into the valuable bio-EG platform chemical [81–84].

A series of works have been done on the conversion of (hemi) cellulose to EG over tungsten carbide catalysts, which was summarized in Table 1. The dispersion of transition metal carbides has a virtual influence on the product selectivity. The tungsten carbides in previous reports were prepared by the solid-solid phase reaction [79], which operated at ca. 1000 K. The tungsten carbide particles were randomly distributed with particle size of 5–80 nm. To improve the dispersion of tungsten carbide particles on supports, Ji et al. modified the co-impregnation method to the post-impregnation method. The particle size of catalysts was greatly decreased to be less than 10 nm. Consequently, the EG yield was elevated to 73.0% with a 100% conversion of cellulose [85]. Zhang et al. used the high surface area MC as the support to load the tungsten carbide for cellulose conversion. The tungsten carbide particles obtained were uniformly distributed at ca. 10 nm, which led to an EG yield up to 72.9% in cellulose conversion [37]. The formation of tungsten carbide promoted by Ni was monitored by Rodella et al. during the carburization process. It was found that the Ni promoter lowered the carburization temperature and protected carbides surface from phase changes by the *in situ* formed carbon. Although the conversion of cellulose was decreased, the Ni promoted tungsten carbides showed a relatively higher stability under reaction conditions [86]. In contrast, Leal et al. used Pt to modify the carbide catalysts, which hindered the excessive carbon deposition on the catalyst during the carburization process. The resulted catalysts demonstrated both higher cellulose conversions and EG yield compared with the non-promoted or Ni promoted tungsten carbide catalysts [87]. To achieve both high activity and stability of metal carbide catalysts under hydrothermal conditions, many promising works have being done recently to balance the carbon on the surface of carbides and/or maintain the phase of carbides with noble metals [35,88].

Given their high activity in conversion of cellulose to EG, tungsten carbide catalysts have also been widely used in other carbohydrates conversion such as sugars, hemicellulose, and raw or pretreated biomass. Ooms et al. converted concentrated sugar to EG in a fed-batch system over Ni promoted tungsten carbide catalysts. Through adjusting the composition of catalysts and the parameters of the reaction, the culminated EG yields reached 66% with a volume productivity of ca. 300 $g_{EG}\ L^{-1}\ h^{-1}$ [89]. Zhou et al. prepared a series of Ni-W_2C/AC catalysts for Jerusalem artichoke tuber conversion, and obtained 38.5% yield to 1,2-PG over a 4%Ni–20%W_2C/AC catalyst within 80 min at 518 K and 6 MPa H_2. They also proposed the possible reaction networks for glucose and fructose based feedstocks over tungsten carbide catalysts [90]. From the application point of view, Pang et al. used corn stalk for catalytic conversion over Ni-W_2C/AC catalysts. Results showed that both the hemicellulose and cellulose were converted to EG efficiently. However, the lignin is detrimental to the catalysts for cellulose conversion. Some pre-processes are suggested to remove the lignin for an efficient conversion of (hemi)cellulose to EG [91,92]. Similarly, Fabičovicová et al. used ethanol/water solution to remove the lignin in straw for further catalytic conversion. With this pretreatment, the EG yield increased from 3% (raw barley straw) to 63–70% over Ru-W/AC catalysts [93,94].

It is worth mentioning that the soluble tungstic species, i.e, soluble tungsten bronze, are active for the retro-aldol condensation reaction (C—C bonds cleavage), as in detail discussed in previous papers [27,82,95]. Those soluble tungsten species when mixed together with hydrogenation catalysts could form bifunctional catalysts such as Raney Ni-H_2WO_4) and Ru/C–H_2WO_4 for EG production [95,96]. In contrast, the tungsten carbide catalysts can solely fulfill the retro-aldol condensation and hydrogenation reactions for EG production [27].

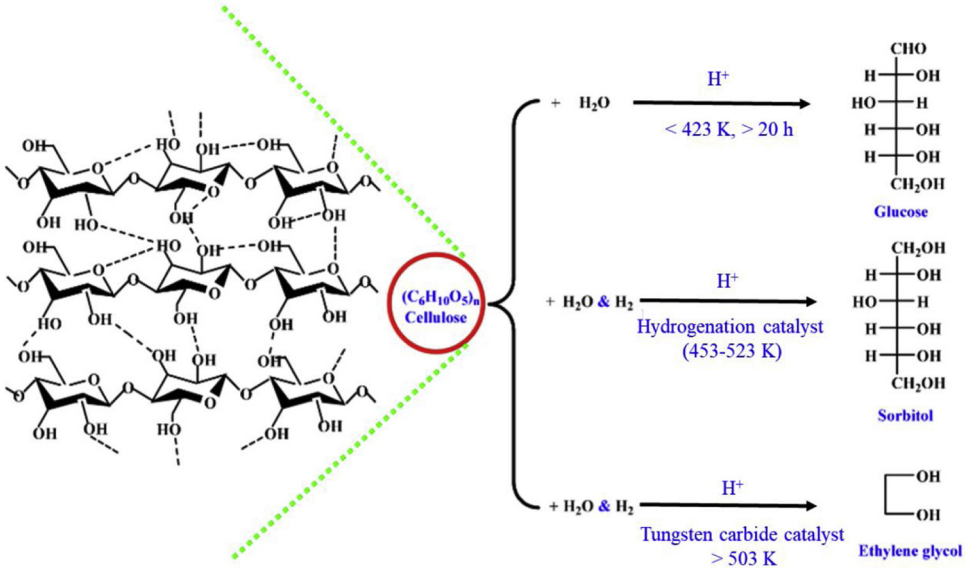

Fig. 7. Catalytic conversion of cellulose to different products [27].

Table 1
Catalytic conversion of (hemi)cellulose over typical carbides and comparison catalysts.[a]

Catalyst	Reaction Conditions	Main products	Yield/%	Ref.
W_2C/AC	cellulose, batch reactor, 6 MPa hydrogen, 518 K, 30 min	EG	27.4	[79]
Ni-W_2C/AC		EG	61.0	
Pt/AC		EG	8.2	
Ni-Mo_2C/AC		EG	11.3	[80]
Ni-(W_2C/AC)		EG	73.0	[85]
WC_x/MC		EG	72.9	[37]
Ni-WC_x/MC		EG	74.4	
Pd-W_2C/C	cellulose, batch reactor, 4 MPa hydrogen, 493 K, 150 min	EG	58.2	[87]
Ni-W_2C/AC[b]	glucose, fed-batch reactor, 6 MPa hydrogen, 518 K	EG	66.0	[89]
Ni-W_2C/AC	jerusalem artichoke tuber, batch reactor, 6 MPa hydrogen, 518 K, 80 min	1,2-PG	38.1	[90]
		EG	14.1	
Ni-W_2C/AC[c]	corn stalk, batch reactor, 6 MPa hydrogen, 518 K, 150 min	EG	32.0	[91]
Ru-W/AC[d]	barley straw, batch reactor, 6.5 MPa hydrogen, 493 K, 3 h	EG	63–70	[93,94]

[a] EG and 1,2-PG are abbreviations of ethylene glycol and 1,2-propylene glycol, respectively. The hydrogen pressure was measured at the room temperature.
[b] the aqueous glucose was feeding into the reactor by a pump, and the final volume productivity reached 300 $g_{EG}\ L^{-1}\ h^{-1}$.
[c] the corn stalk was pretreated by ammonia and H_2O_2.
[d] the barley straw was pretreated by the ethanol/water mixture, and the hydrogen pressure was measured at the reaction temperature.

3.2. Catalytic conversion of lignin over transition metal carbides

Lignin is the second most abundant renewable source in plant cell, which has a three dimensional structure that fills the spaces between cellulose and hemicellulose. It forms a rigid structure with (hemi) cellulose that is hard to be degraded under most chemical and bio-conditions. Additionally, the depolymerized lignin fractions are prone to be re-polymerized under the reaction conditions. Hence, it is still a challenge to depolymerize lignin into target phenols efficiently. After years of exploration, enzymatic depolymerization, pyrolysis, oxidation and hydrotreating methods have been developed to unlock the structure of lignin for chemicals or fuels production [28,97–101]. Enzymatic depolymerization employs bacterial enzymes for lignin breakdown under mild conditions [97]. In contrast, pyrolysis conducts in harsh reaction conditions (> 623 K) in the absence or presence of catalysts, producing a range of aromatics [102,103]. The oxidation and hydrotreating processes happen at moderate temperatures (453–573 K) with the assistance of robust catalysts [104]. Besides the acid, base and metals catalysts, transition metal carbide catalysts, typically tungsten and molybdenum carbides, have showed high potential for the lignin conversion, which demonstrated high selectivity towards β-O-4, α-O-4, β-β and 4-O-5 bond cleavages, as shown in Fig. 8 [28].

During the raw biomass conversion process, Li et al. found that Ni-W_2C/AC catalysts not only converted the (hemi)cellulose to glycols but also promoted the lignin conversion. The lignin in biomass was selectively converted to monophenols with a yield of 46.5% in water under hydrothermal conditions [105]. Then, they conducted the reaction using model compounds and lignin, and confirmed that the W_2C/AC catalysts showed high activity to β-O-4 cleavage, α-O-4 and β-β bonds deconstruction. These bonds dominated the linkage between units in lignin (Fig. 8). Therefore, a yield of 96.8% to C–O cleavage products from model compounds and 70.7% to liquid oils from the lignin were obtained under 0.69 MPa hydrogen in methanol solution at 533 K [106]. The same group also investigated the influence of lignin types on its catalytic conversion over tungsten carbide catalysts. They isolated different types of lignin from grassy and woody materials, and found that Klason and alkaline lignin had more resistant structures to be degraded, whereas organosolv lignin had the similar structure to the native lignin that was liable to be depolymerized. Meanwhile, the softwood lignin possesses higher molecular weights than the hardwood lignin, and corn stalk lignin has the lowest molecular weight because of its relatively shorter growth period [107].

Besides the tungsten carbides, molybdenum carbides also showed high activity for lignin conversion. A series of studies for lignin

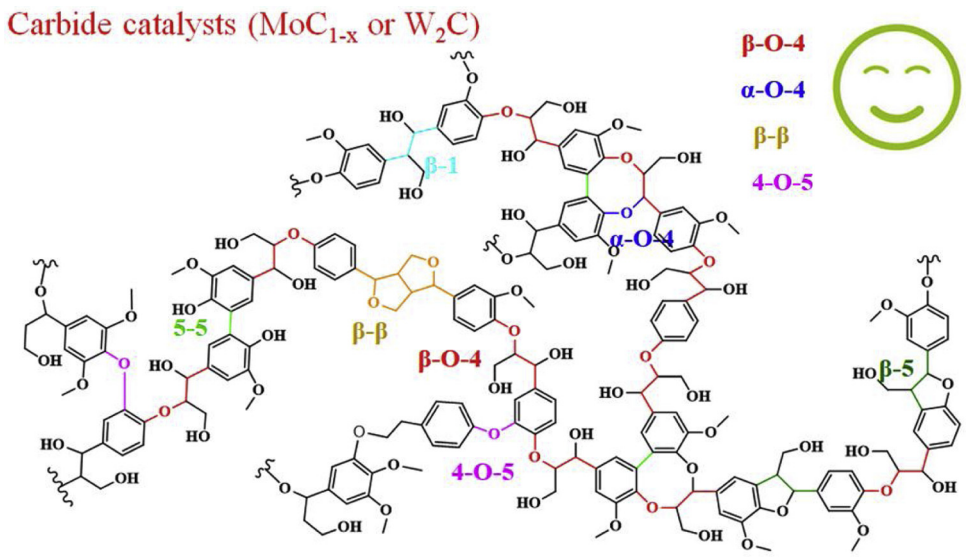

Fig. 8. Typical transition metal carbides for lignin conversion.

conversion have been done over molybdenum carbide catalysts in Li's group [108–111]. Ma et al. directly used Kraft lignin as the feedstock to produce high-value small-molecular chemicals in supercritical ethanol over α-MoC_{1-x}/AC catalysts. About 25 low molecular weight compounds including C_6–C_{10} esters, alcohols, arenes, phenolics, and benzyl alcohols were obtained with the overall yield of 1.64 g liquid products per gram of lignin [108]. The same group also investigated the role of Mo in the catalytic degradation of lignin in an ethanol solution. They compared metallic molybdenum, carbide, and nitride for this reaction, and found that Mo carbide and metallic catalysts gave a higher overall yield. During the reaction, Kraft lignin is first degraded via a non-catalytic ethanolysis process. Then, the main active Mo(V) species dissociated from the solid catalyst, acting as active species to further convert the segments into small molecules [109]. Based on the reaction routes, they developed a series of MoC_{1-x}/Cu-$MgAlO_z$ catalysts for lignin conversion, which showed a higher activity to aromatic compounds with 575 mg/g lignin at 603 K. Additionally, the catalysts have been reused at least five times with a 22.4% loss in the yield to aromatic compounds [110]. They also used the reaction intermediate, guaiacol, as the feedstock for catalytic conversion, trying to unravel the intrinsic mechanisms for this highly active molybdenum carbide catalyst. It was found that the carbide catalysts were very active for the demethoxylation and trans alkylation reactions, which converted the guaiacol to phenol and alkylphenols with an 85% combined selectivity at 87% conversion in ethanol solution. In contrast to most metal catalysts that produce ring-saturation products (i.e., cylclohexane based products) [112], transition metal carbides were potential catalysts for the selective conversion of lignin to phenolic compounds [111]. Cattelan et al. also reported that Mo_2C catalysts exhibited the highest selectivity to aromatic compounds in the lignin depolymerization process with supercritical ethanol as the reaction medium. Under the reaction conditions, the H was transferred from ethanol to lignin oligomers over the carbide catalysts, which generated a low accessible H micro-environment that inhibited the excessive hydrogenation of the aromatic ring. Therefore, renewable aromatics were preferentially produced [113]. Similarly, due to the minimized C—C bonds re-coupling in the ethanol and water medium, the highest lignin monomer yield of 37.3% was obtained from the corn stover lignin over the bulk Ni-Mo_2C catalyst [114].

In summary, transition metal carbide catalysts have been widely applied in the lignin conversion, and demonstrated to be highly selective to phenolics. However, this application is only limited to tungsten and molybdenum carbides. With the development of novel preparation methods, other transition metal carbides with special sites or structures could also be promising for lignin conversion. Additionally, it is still a challenge to cleave the C—C and some C–O—C bonds in lignin over the present carbide catalysts. Multiple active sites including metal, acid or base should be combined into the catalysts for lignin conversion.

3.3. Catalytic conversion of platform chemicals over transition metal carbides

Due to the complex and rigid structure of biomass, it is still highly challenging to directly convert biomass or main components of biomass to fuels or chemicals. Generally, multiple steps are always employed to bridge the gap between biomass and finally products. Sometimes, the catalytic or enzymatic processes are integrated to fulfill this goal. For instance, biomass is first converted to pyrolysis oil or oxygen-containing chemicals by thermal chemistry or fermentation processes, and then the oil or chemicals are further refined to fuels via the deoxygenation reaction [6,115].

3.3.1. Selective deoxygenation of platform chemicals to fuels

Generally, the biomass derived chemicals have more oxygen contents than the prevailing fossil fuels. Therefore, the deoxygenation process has been extensively investigated. A series of catalytic materials have been studied for the biomass derived chemicals upgrading, including zeolites, supported metal catalysts, transition metal nitrides and carbides [3,29,116–119]. Among those achievements, transition metal carbides have been proved to be efficient for a variety of feedstocks, particularly for organic acid/ester and phenolics [68].

Triglyceride-based biomass is one of the most important renewable energy resources, which has the similar structure to hydrocarbons. However, further reactions were needed to remove the carboxyl or ester groups to satisfy the modern diesel engines. Transition metal carbide catalysts have showed high selectivity to the deoxygenation of fatty acids (Table 2). Han et al. supported nanostructured molybdenum carbides on multi-walled carbon nanotubes (Mo_2C/CNTs) for vegetable oils deoxygenation. The carbide catalysts were demonstrated to possess higher activity and selectivity to branched diesel-like hydrocarbons (57%) compared with noble metals (i.e., Pt, Pd) [38,120]. Then, they compared different phases of molybdenum carbide (Mo_2C, MoC) for hydrodeoxygenation of vegetable oils. The MoC supported on ordered mesoporous carbon demonstrated 85–95% selectivity to diesel-like hydrocarbons [121]. By doping the mesoporous carbon with nitrogen, Wang et al. found that the Mo dispersion was improved over the Mo_2C/

Table 2
Deoxygenation of fatty acids over typical transition metal carbide and comparison catalysts.[a]

Catalyst	Reactant	Reaction Conditions	Product and yield	Ref.
Mo_2C/CNTs	methyl palmitate	batch reactor,, 513 K, 2 h, 1.5 MPa hydrogen	hexadecane; 57%	[38]
Pd/CNTs			pentadecane; 84%	
MoC/OMC	vegetable oil	batch reactor,, 533 K, 2 h, 1.5 MPa hydrogen	hydrocarbon; 95%	[121]
Mo_2C/N1.0MC	fatty acids	batch reactor,, 623 K, 3 h, 3 MPa hydrogen	alkane liquid; 80.4%	[122]
W-600 (WO_3)	stearic acid	batch reactor,, 623 K, 5 h, 5 MPa hydrogen	n-C_{17}; 25%	[123]
W-1000 (W_2C)			n-C_{18}; > 50%	
Mo_2C/RGO	oleic acid	fixed bed reactor, 623 K, H_2/reactant = 4.5	hydrocarbon; 84.5%	[126]
β-Mo_2C/CNF	stearic acid	batch reactor,, 573 K, 2 h, 5 MPa hydrogen	C_{18}; 73.5%	[127]
α-MoC_{1-x}/CNF	stearic acid	batch reactor,, 623 K, 6 h, 6 MPa hydrogen	C_{18}; > 80%	[128]
NiMoC/Al-SBA-15	soybean oil	fixed bed reactor, 673 K, 6.5 MPa hydrogen LSHV = 1^{-1}	hydrocarbons; 97%	[129]

[a] CNT, OMC, MC, ROG, CNF and LHSV are abbreviations of carbon nanotube, ordered mesoporous carbon, mesoporous carbon, reduced graphene oxide, carbon nanofiber and liquid hourly space velocity, respectively.

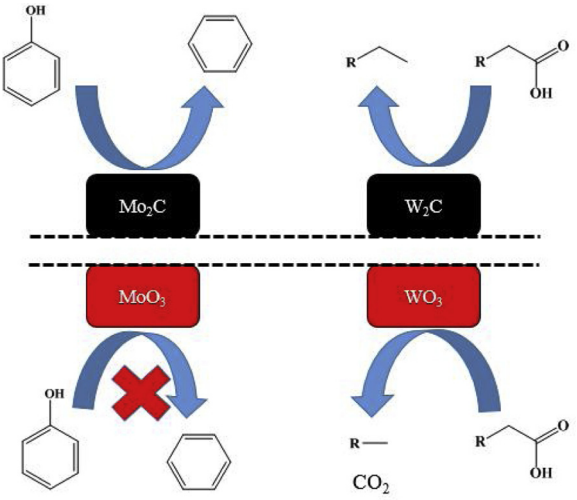

Fig. 9. Different reaction pathways for bio-chemical conversions over transition metal carbide and oxide catalysts [123,124].

N1.0 mesoporous carbon catalyst, and correspondingly enhanced the diesel-like alkane liquid to 80.4% [122]. Gosselink et al. studied the performance of tungsten based catalysts at different reduction temperatures for the deoxygenation of the triglyceride/fatty acid. As shown in Fig. 9, decarboxylation/decarbonylation dominants over the supported tungsten oxides reduced at low temperatures, whereas hydrodeoxygenation prevails over the supported tungsten carbide catalysts. The similar trend was also observed over the Mo-based catalysts, where the phenol was solely converted to benzene over carbide catalysts [123–125]. Kim et al. supported Mo_2C on various carbons for the deoxygenation of oleic acid and soybean oil to produce diesel-range hydrocarbons. Over the uniformly distributed Mo_2C nanoparticles, ≥ 85% yield and ≥ 90% selectivity to hydrocarbons were achieved at 623 K, a hydrogen pressure of 5.0 MPa and a H_2/oil ratio of 4.5 [126]. Suitable particle size or carbide phases are essential to the high activity and stability of carbide catalysts in the deoxygenation reactions. Stellwagen et al. reported that relatively large particles of carbides (10 nm) are more stable under the reaction conditions, and smaller particles (3 nm) were prone to be oxidized and thus lost its activity in the recycle runs [127]. Macedo et al. compared α-MoC_{1-X}/CNF and β-Mo_2C/CNF catalysts for the hydrodeoxygenation of stearic acid. Due to the more accessible Mo atoms at the surface of the α-MoC_{1-X} phase, it demonstrated higher weight performance than the β-Mo_2C/CNF counterpart [128]. Certain metal additives have been introduced to prevent the smaller carbide particles from oxidization with elevated reactivity. For instance, Wang et al. prepared the NiMoC/Al-SBA-15 catalysts for the hydrotreating of soybean oil. The carbides demonstrated high activity (100% conversion and 97% selectivity to green diesel) and stability (7 days), which was attributed to the fine carbide particles (5 nm), large surface area supports, and promotion effect of Ni on the stabilization of carbide against oxidation [129].

Other than the abovementioned fatty acid, metal carbide catalysts have also been used in deoxygenating acetic acid due to its large amounts of production during the biomass pyrolysis process. Schaidle et al. conducted the deoxygenation of acetic acid over carbide catalysts (Mo_2C). At the temperature range of 523–673 K, C–O bonds cleavage products of acetaldehyde and ethylene were selectively formed, which was attributed to the acid and metal sites of carbides that determined the C—O bond cleavage steps and the deoxygenation rate, respectively [130]. The results were also proved by Sullivan et al. during the investigation of acetone deoxygenation over Mo_2C catalysts. They concluded that the high activity of metal carbides in selective deoxygenation should be attributed to the bifunctional metal and acid sites that responsible for hydrogenation and dehydration of the carbonyl groups [131].

Beyond the hydrodeoxygenation of carboxyl groups in organic acids, transition metal carbide catalysts have also been employed to upgrade the pyrolysis oils with abundant phenolics. Jongerius et al. used a two-step approach for the conversion of lignin to monoaromatics. They first depolymerized lignin in a liquid phase reforming reaction, and then hydrodeoxygenated the isolated lignin-oil to aromatics. Over the Mo_2C/CNF catalyst, highest aromatic yields and lowest oxygen content were obtained from the lignin derived liquids, which is consistent with the results for guaiacol conversion [132,133]. Chen et al. explored the catalytic performance of W_2C/MCM-41 in lignin fast pyrolysis. They found that the metal carbide catalysts showed excellent selectivity to monocyclic arenes. During the pyrolysis process, 20% yield to arenes were obtained at 1023 K with the selectivity being up to 85% [134]. In accordance with these results, carbide catalysts were found to be significantly promoted the hydrodeoxygenation of phenolics during the conversion of biomass to fuels [135,136]. The reaction pathway of phenol hydrodeoxygenation was calculate over β-Mo_2C (110) catalysts by Engelhardt et al. [137]. As shown in Fig. 10, the direct deoxygenation route (DDO) proceeds in C–O and surface C–H bonds cleavage, along with simultaneously formation of benzene and surface Mo-O bonds (a stand-up adsorption geometry of phenol on the Mo_2C@2H surface). This pathway has a low activation barrier of 1.2 eV, which is energetically preferable to benzene production. In contrast, the hydrogenation (HYD) pathway has a much higher reaction barrier (> 2.2 eV) than that of the DDO pathway, in which the phenol adsorption first changed from a stand-up to a flat arrangement, followed by the hydrogenation of the C1 carbon, and then that of the C atom in *ortho* position. Therefore, the selectivity to benzene reached 85% for phenol conversion over the MoC_x/HCS (hollow carbon spheres) catalyst.

To unveil the intrinsic properties of metal carbides, some typical model compounds with multi-functional groups including guaiacol, phenol, anisole, and benzofuran were also investigated. As shown in

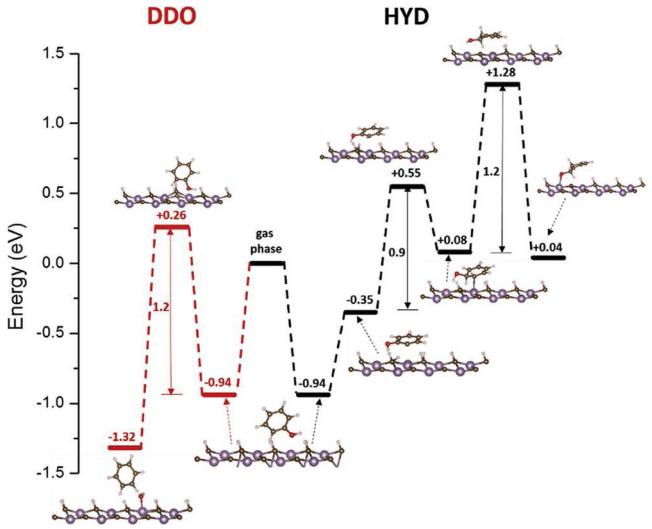

Fig. 10. Reaction energy profiles of phenol conversion via direct deoxygenation route (DDO) and hydrogenation (HYD) pathways over the Mo_2C@2H surface. Two hydrogenation steps are described in the HYD route: C1 is hydrogenated first, followed by hydrogenation in the *ortho* position [137].

Table 3, Fang et al. synthesized a series of tungsten carbide catalysts (W_xC@ carbon spheres) for guaiacol conversion, which showed a particularly selective cleavage of aryl C—O bonds even at a 573 K and a high H_2 pressure of 3 Mpa [138]. To get the high activity in hydrodeoxygenation of guaiacol, high carburization temperatures and low heating rates were needed to remove the surface inactive oxycarbide phases [139]. Boullosa-Eiras et al. screened titanium-supported molybdenum carbide, nitride, phosphide and oxide catalysts for hydrodeoxygenation of phenol. The 15 wt% Mo_2C/TiO_2 showed the highest selectivity (> 90%) to benzene at 623 K and 25 bar of hydrogen [140]. Lee et al. employed the anisole as a feedstock for deoxygenation on molybdenum carbide catalysts. The bulk catalysts demonstrated 94% selectivity to benzene (C_{sp2}–O bond cleavage) with less than 9% cyclohexane [141]. The same reaction was also conducted by Iida et al. over encapsulated MoCx nanoclusters in the zeolite of faujasite. Alkylated aromatics (toluene and xylene) were preferentially produced with minimized CH_4 formation, which was attributed to the synergistic effect of Brønsted acid and metal sites for the trans alkylation reactions over the confined carbide catalysts [142]. Liu et al. found that the reaction pathway for hydrodeoxygenation of 2-methoxyphenol differ greatly between noble metals and carbides. Over the molybdenum carbide catalysts, the reaction occurs by direct demethoxylation yielding phenol followed by Ar − OH bond cleavage to ultimately yield benzene, rather than ring saturation toward cyclohexane products observed over noble metal catalysts (Fig. 9) [143]. Recently, Liu et al. synthesized W_2C nanorods by an organic–inorganic hybrid strategy for the catalytic hydrodeoxygenation of benzofuran, and simultaneously investigated the hydrogenation, hydrogenolysis and deoxygenation reactions. They concluded that the abundant defects in tungsten carbides that derived from the deficiency of carbon atoms should be the main reason for the excellent scission effect on C_{ar}–O cleavage for producing unsaturated aromatics [144]. Different from noble metal catalysts, the main products for the deoxygenation of these model compounds are unsaturated alkenes or benzene based compounds instead of saturated alkanes, which both improves the products value and reduces the overall H_2 consumption [145–148].

Additionally, the carbide catalysts have been widely used in upgrading other biomass derived chemicals. Chen's group developed a series of carbide catalysts with different structures to study the unique role of transition metal carbides in the conversion of biomass derived oxygenates. After a combination of density functional theory (DFT), surface science investigation, and catalytic reactivity studies, they found that carbide catalysts such as Mo_2C are highly selective deoxygenation catalyst in upgrading small molecule like ethanol, propanal, and more complex biomass derived molecules like furfural [149–152]. For furfural, a model compound contains carbon–oxygen bonds both outside and inside the furan ring, they first compared the binding energy and bond lengths of furan, 2-methylfuran, and furfuryl alcohol on a close-packed Mo_2C (0001) surface via DFT calculations, and predicted that the furfural is likely to be deoxygenated on the outside the furan ring due to the strong η_2(C,O) adsorption of furfural and thus weakened C1 = O1 bond (carbon–oxygen bonds outside the furan ring) on the Mo_2C surface. High resolution electron energy loss spectroscopy was further used to confirm the configuration of furfural adsorption over the model Mo_2C surface. Powder Mo_2C catalysts were also synthesized and tested for furfural conversion. About 60% selectivity to 2-methylfuran was obtained, which confirmed that transition metal carbides are efficient catalysts for the selective deoxygenation of biomass derived furfural [152]. Recently, the same group employed Co or Fe to modify Mo_2C for furfural hydrodeoxygenation. The introduction of Co or Fe reduced the binding energy between oxygen and furfural, which promoted the removal of surface oxygen on carbide and then improved the stability of carbide catalysts [153,154]. Similarly, Shi et al. revisited the hydrogenation of furfural over clean and 4H pre-covered Mo_2C(101) surfaces. Two distinct surface sites of unsaturated C_A (4-coordinated) atoms and unsaturated Mo_A (10-coordinated) atoms were identified for H and furfural adsorption, respectively. The furfural − CHO is preferring adsorbed at the Mo_A site, which has a minimum energy pathway to 2-methylfuran at high hydrogen pressure [155]. McManus and Vohs studied the adsorption and reaction of glycolaldehyde and furfural on a model catalyst of Mo_2C/Mo(100). Glycolaldehyde and furfural interacted with Mo_2C/Mo(100) surface via the aldehyde functional group, which had an η1(O) configuration at < 200 K and changed to di-σ η2(C,O) configuration at 200–300 K. The bonding configuration changes weakened the C–O bond in the carbonyl groups, which was considered as the main reason for the hydrodeoxygenation of aldehyde functional groups, rather than furan rings [156].

Table 3
Deoxygenation of typical model compounds over transition metal carbide catalysts.[a]

Catalyst	Feedstock	React conditions	Product and yield	Ref.
WxC@carbon sphere	guaiacol	fixed bed reactor, 573 K, 3.0 MPa H_2, WLHSV = 3.0 h^{-1}	phenol; 92.5%	[138]
Mo_2C/CNF	guaiacol	batch reactor, 623 K, 2 h, 3 Mpa H_2	phenol based compounds; 91.8%	[145]
Mo_2C/TiO_2	phenol	fixed bed reactor, 623 K, 2.5 MPa H_2	benzene; > 90%	[140]
Mo_2C	anisole	fixed bed reactor, 423 K, ~0.1 to ~1 atm H_2	benzene; 94%	[141]
MoC_x/FAU	anisole	fixed bed reactor, 523 K, AP, $P_{anisole}$ = 0.0079 bar	phenolic compounds; > 70%	[142]
Mo_2C/AC	2-methoxyphenol	batch reactor, 3.4 MPa H_2, 623 K, 6 h	phenol; > 90%	[143]
W_2C nanorod	benzofuran	fixed-bed reactor, 613 K, 4 MPa H_2	mainly ethylbenzene	[144]
β-Mo_2C	furfural	flow reactor, AP, 423 K	2-methylfuran; 50–60% selectivity	[146]
porous Mo_2C	propanal	flow reactor, AP, 573 K	propylene; > 60% selectivity	[150]

[a] WLHSV, CNF and AP are abbreviations of weight liquid hourly space velocity, carbon nanofiber, atmospheric pressure, respectively.

The reaction medium or conditions also greatly affected the reaction pathway. In the case of butanol solvent, the α-MoC catalysts were covered by four alkoxides derived from 2-butanol dissociation, which promoted the furfural hydrogenolysis to 2-methyl furan. In contrast, the alkoxide species on the surface of the α-MoC catalysts increased to six in the methanol solvent, which sterically inhibited the −OH removal to produce furfuryl alcohol. Such solvent-induced surface modification of carbides provided a convenient way for controlling the distribution of hydrodeoxygenation products [157]. During the synthesis of bio jet fuels from 2-methylfuran, acetone and butanal, Li et al. first coupled 2-methylfuran with acetone and butanal, respectively, over Nafion-212 resin catalysts via the hydroxyalkylation/alkylation reactions, and then hydrodeoxygenated the hydroxyalkylation/alkylation intermediates to fuels over the Ni-W_xC/AC catalysts. It was found that the Ni-W_xC/AC catalyst exhibited better catalytic performance and stability than noble metals in the hydrodeoxygenation reactions, which was attributed to the multiple active sites of Ni promoted tungsten carbide catalysts [158]. By adjusting the reaction conditions and catalysts, the oxygen groups both in and out of furfural rings can be deoxygenated in the presence of transition metal carbide catalysts, which provides high potential for the selective deoxygenation of biomass to fuels.

3.3.2. Selective conversion of platform chemicals to fine chemicals

As above mentioned, transition metal carbides have been widely used for deoxygenation model compounds, which provide solid foundations for converting biomass to fuels. Besides of that, these achievements also stimulate the conversion of platform chemicals to fine chemicals. Some excellent reviews summarized the recent progresses in upgrading biomass to chemicals over carbide catalysts [29,68,147]. Herein, we show several typical examples in deoxygenation and dehydrogenation reactions to show the special activity of transition metal carbide catalysts.

Transition metal carbide catalysts were primarily used for the conversion of furan based chemicals. Rogowski et al. synthesized the W_xC-β-SiC nanocomposite powders by the carbothermal reduction method for furfural hydrogenation. Given the harsh preparation conditions used, the resulted catalysts had a large particle size (15–40 nm) and low surface area (< 30 m^2/g). Although a yield of 90% to tetrahydrofurfuryl alcohol was achieved, the efficiency of the catalysts is low given that a low concentration of furfural (0.1 mol/L) and a high catalyst/feedstock ratio (ca. 2:1) was employed [159]. It is still highly demanded to further improve the reaction efficiency of transition metal carbide catalysts by improving the synthesis. Recently, Huang et al. prepared nickel promoted tungsten carbide catalysts for the selective hydrogenation of 5-(hydroxymethyl)furfural (HMF), and achieved a 96% yield to 2,5-dimethylfuran at 453 K. As shown in Fig. 11, different reaction pathways were proposed over the Ni and Ni promoted tungsten carbides. Over Ni catalysts, random hydrogenation products (i.e., 2,5-dimethyltetrahydrofuran, furfural alcohol and 2,5-dimethylfuran) was obtained. On the contrary, 2,5-dimethylfuran was selectively produced over the Ni-W_2C/AC catalysts. Although the tungsten carbide (W_2C) exhibited good deoxygenation activity, the synergy between Ni and W_2C was believed to be critical for maintaining the high selectivity to 2,5-dimethylfuran over the Ni-W_2C/AC catalysts [160]. To increase the reaction efficiency, Braun et al. used a simple cascade flow reactor loaded with Amberlyst 15 and Ni@WC catalysts for one-pot conversion of fructose to 2,5-dimethylfuran, which led to a yield of 38% to dimethylfuran and 47% to ethyl levulinate in 20 min [161].

Transition metal carbides also showed attractive activity for the conversion of levulinic acid into γ-valerolactone, a top value added chemicals from biomass [162,163]. Mia et al. used the carbon supported Mo_2C catalyst to convert levulinic acid into γ-valerolactone. It is observed that both the support and location of the carbides played a pivotal role in maintaining the activity and stability of molybdenum carbide catalysts. The carbon nanotubes supported Mo_2C catalyst gave higher activity and stability than the active carbon supported counterparts did. Notably, when the carbides are located within the carbon nanotubes, 99% conversion and 90% selectivity to γ-valerolactone were achieved at 473 K and 30 bar H_2 in a continuous-flow trickle-bed reactor [164]. Quiroz et al. synthesized a series of Mo_2C catalysts for the hydrogenation of levulinic acid to produce γ-valerolactone. The β-Mo_2C 1D nanostructures presented a relatively higher activity than other phases of carbide (> 85% selectivity), which can be correlated with the number of the sites measured by the CO uptake [165].

Recently, Dai et al. reported the production of *para*-xylene from 4-methyl-3-cyclohexene-1-carbonylaldehyde (derived from the bio chemicals of acrolein and isoprene) over tungsten carbide catalysts. The W_2C was found to be selective for the intramolecular hydrogen transfer and C=O bonds dissociation during the dehydro-aromatization–hydrodeoxygenation cascade process, leading to the high yield to *para*-xylene (> 94%) without using an external hydrogen source [166].

4. Outlook

Great progresses have been made for both the synthesis and application of transition metal carbides in biomass conversion. A variety of bottom-up construction strategies have been developed to control the structure and size of metal carbides, which play an essential role to their applications in this fields. As such, the catalytic conversion of biomass to fuels and chemicals over carbide catalysts has attracted more and more attentions. Different types of carbides including tungsten and molybdenum carbide have been widely used in (hemi)

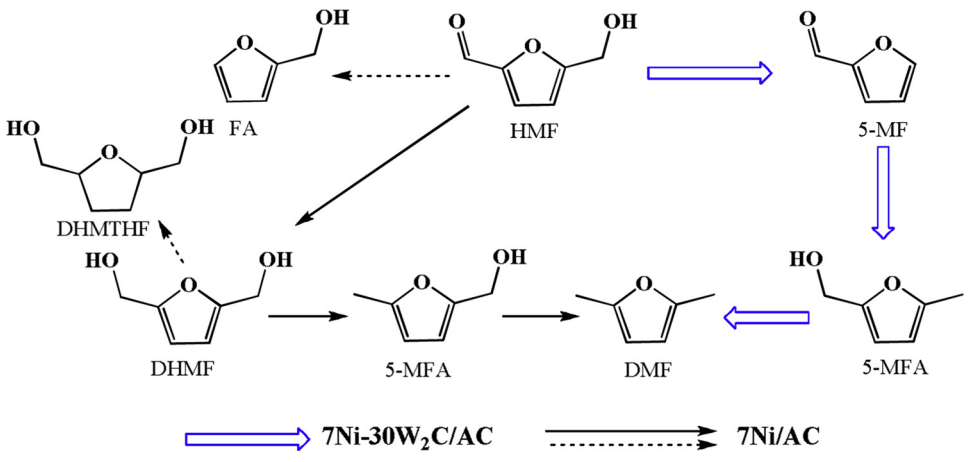

Fig. 11. Possible reaction pathway for the catalytic conversion of HMF over different catalysts (5-MF: 5-methylfurfural; 5-MFA: 5-methylfurfuryl alcohol; DMF: 2,5-dimethylfuran; DHMF: 2,5-dihydroxymethylfuran; DMTHF: 2,5-dimethyltetrahydrofuran; FA: furfural alcohol) [160].

cellulose, lignin and platform chemicals conversion, and some carbides have been demonstrated to be highly selective in hydrodeoxygenation reactions. However, despite of the potential of transition metal carbides in the upgrading of biomass and/or biomass derived chemicals, challenges still exist in both the catalysts synthesis and the application in catalytic biomass upgrading.

1) Synthesis of highly dispersed and stable metal carbide catalysts. Great efforts have been made to improve the synthesis method, including the control of the particle size, phase structure, and stability of carbide catalysts [167]. However, the synthesis of highly disperse transition metal carbides nanoparticles (i.e., 1–5 nm) is still limited to special synthesis protocols such as using confinement of nonporous supports. Preparing highly dispersed metal carbide with high activity and stability is still challenging. Currently, the prevailing carbide catalysts are still prepared at high temperatures, which caused the irreversible particle aggregation.

The solid-solid phase reaction has a long history, but it is conducted at high temperatures, and it is very difficult to control the carburization process [9]. Although the method was improved to some extent by changing the metal precursors and employing high surface area carbon precursors [36], the particle size of most metal carbides reported is still larger than 5 nm. In contrast, the liquid derived solid-solid phase reaction shows a great potential to control the particle size of finally carbides [51]. Especially, the liquid phase provides a versatile media for the controllable synthesis of the precursors, which significantly improved the dispersion of carbides to 1–5 nm. The solid-gas phase reaction, i.e., temperature program reduction method, is relatively mature, which has been widely used for preparing different carbides. Nevertheless, it still has the drawback of carbon depositions.

1) Synthesis of high purity carbide catalysts. The carbide prepared by traditional methods always have the problems of surface carbon deposition, and even a mixture of different carbide phases, making the correlation of structure-functionality of metal carbide catalysts difficult. Extensive efforts have been being made to control the phase and surface structure of metal carbides [168]. One of the promising way is exposing the clean metal surfaces to unsaturated hydrocarbons and then annealing at certain temperatures. Pure carbides with controllable carbon/metal ratios could be synthesized, which builds a solid foundation for the reaction mechanisms study [169]. Additionally, besides the commonly synthesized carbides, some non-stoichiometric carbide with special defects, or unique structure carbides have been proved to have special activities in biomass conversion [170–172]. These achievements will guide the transition metal carbide catalysts synthesis for the biorefinery process.
2) Stability of metal carbide in biomass conversion. The stability of metal carbide is crucial for its applications. Many factors, such as oxidation, particle aggregation, coke formation and leaching, affect the stability of carbides, as previously discussed by Macedo et al. [173]. Transition metal carbides are very sensitive to oxygen containing compounds. The presence of high pressure water inhibited the adsorption of the reactant, and induced the irreversibly deactivation [137]. Similarly, the introduction of oxygen, water and carbon dioxide significantly decreased the toluene formation rates in *m*-cresol hydrodeoxygenation over Mo_2C catalysts [174]. To maintain the high activity of carbides, different strategies have been proposed. For instance, some researches modified the carbide with noble or transition metals and operated the reaction under high pressure hydrogen, which promotes the activation of the hydrogen with the increased H*-site and prevents the carbide from oxidation as proved by experimental results and DFT caculations [175–179]. Besides, many new methods such as modification of the carbide surface to be hydrophobic and spatial confined carbides have been proposed to stabilize carbide catalysts, which shows high potential for biomass conversion [52,180–182].
3) Transition metal carbides for some novel reactions in biomass conversion. As we discussed, carbide catalysts demonstrated unique reactivity in cellulose, lignin and platform chemicals conversions. Tungsten carbides selectively converted carbohydrates to glycols (i.e., EG and PG), which had a high selectivity to EG (WCx 75% EG yield) [82]. Moreover, it shows promising selectivity in the hydrodeoxygenation of lignin derived phenolics. Different from most of metals showing high activity for aromatic ring saturation, the transition metal carbide catalysts selectively cleavage the C_{sp2}-O without consuming extra hydrogen [29]. In spites of these achievements, the application of carbides catalysts in biomass is still needs to be exploited. For instance, more traditional carbide catalysts such as Re, Ti, V or Zr carbides [183] could be explored in the hydrodeoxygenation of bio-chemicals, and some novel structure of carbide like 2D transition metal carbides with preferential exposed facet (MXene) [184,185] could be helpful in fundamental understanding the catalysts in biomass conversion. Additionally, more attempts may be made on the application of carbide in new reactions, especially the reactions concerning weak hydrogen bonds cleavage such as ethanol and alcohols upgrading.
4) The synergistic effect between transition metal carbides and metals. Other than being directly used as catalysts, transition metal carbides could serve an important support for metals, which has been shown promising in other catalytic reactions due to the synergistic effect between metals and metal carbides. For example, atomically dispersed Pt1 (single atom Pt) on α-MoC has been shown highly active for hydrogen production in the aqueous reforming of methanol. Due to the synergistic effect of Pt1 and the maximized active interface of Pt1/α-MoC and α-MoC, the reaction temperature can drop to as low as 423–463 K with an average turnover frequency of 18,046 mol of hydrogen per mole of platinum per hour [24]. In another attempts, the synergistic effect between Au1 (single atom Au) and α-MoC resulted in the high activity of Au1/α-MoC catalysts in water-gas shift reaction at low reaction temperatures (393 K) [186]. These promising results will shed a light on the synthesis and application of the novel carbide in biomass conversion.
5) *in situ* investigations of reaction mechanisms. The conversion of biomass to fuels or chemicals always conducts in the liquid phase, which increases the difficulty in *in situ* characterizations and reaction mechanisms study. With the development of state of the art characterization tools, some characterizations could be conducted under operando or reaction conditions. Recently, *in situ* Attenuated Total Reflection Infra-Red (ATR-IR) spectroscopy has been used in monitoring the reaction process of biomass conversion, which can be conducted at 623 K and 200 bar, covering most reaction conditions in biomass conversion [187,188]. Moreover, sum-frequency generation vibrational spectroscopy (SFG-VS) has been proved as a surface/interface sensitive spectroscopic probe for characterizing the properties of molecular surfaces and interfaces [189]. It will also provide a broad range of information in the catalytic conversion of biomass due to its multi-phase reactions. Some routine instruments have been modified or combined to operando characterizations based on the improved reaction conditions, including the X-ray absorption, FT-IR, Uv–vis, Mössbauer spectroscopy. Very recently, Murugappan et al. used operando near-ambient pressure X-ray photoelectron spectroscopy to unveil the role of MoO_3 and Mo_2C in hydrodeoxygenation of anisole. Different from the MoO_3 catalysts with 5+ and 6+ oxidation states, the Mo_2C showed negligible oxidation state changes and maintained constant 2+ states under the hydrodeoxygenation reaction conditions [190]. Additionally, DFT has been used to model the catalysts based on the *in situ* characterizations, which in turn directed the catalysts design and characterizations. All these efforts will promote the transition metal carbide catalysts design and reaction pathways understanding.

Acknowledgements

This work is supported by the National Natural Science Foundation of China (21690081, 21721004 and 21776268), "Transformational Technologies for Clean Energy and Demonstration", Strategic Priority Research Program of the Chinese Academy of Sciences, Grant No. XDA 21060200. Jifeng Pang acknowledges the support from China Scholarship Council for the Visiting Scholars Program (File No. 201704910436). Junming Sun and Yong Wang would like to thank the financial support provided by US Department of Energy (DOE), Office of Basic Energy Sciences, Division of Chemical Sciences, Geosciences, and Biosciences (DE-AC05-RL01830, FWP-47319).

References

[1] A. Corma, S. Iborra, A. Velty, Chem. Rev. 107 (2007) 2411–2502.
[2] P. Gallezot, Chem. Soc. Rev. 41 (2012) 1538–1558.
[3] C. Liu, H. Wang, A.M. Karim, J. Sun, Y. Wang, Chem. Soc. Rev. 43 (2014) 7594–7623.
[4] J. Sun, Y. Wang, ACS Catal. 4 (2014) 1078–1090.
[5] J.S. Luterbacher, D.M. Alonso, J.A. Dumesic, Green Chem. 16 (2014) 4816–4838.
[6] I. Wheeldon, P. Christopher, H. Blanch, Curr. Opin. Biotechnol. 45 (2017) 127–135.
[7] T. Ennaert, J. Van Aelst, J. Dijkmans, R. De Clercq, W. Schutyser, M. Dusselier, D. Verboekend, B.F. Sels, Chem. Soc. Rev. 45 (2016) 584–611.
[8] R.B. Levy, M. Boudart, Science 181 (1973) 547–549.
[9] S.T. Oyama, Catal. Today 15 (1992) 179–200.
[10] L. Brewer, Science 161 (1968) 115–122.
[11] E. de Smit, B.M. Weckhuysen, Chem. Soc. Rev. 37 (2008) 2758–2781.
[12] L. Ramqvist, K. Hamrin, G. Johansson, U. Gelius, C. Nordling, J. Phys. Chem. Solids 31 (1970) 2669–2672.
[13] S. Ramanathan, S.T. Oyama, J. Phys. Chem. 99 (1995) 16365–16372.
[14] M.J. Ledoux, C. Pham-Huu, R.R. Chianelli, Curr. Opin. Solid State Mater. Sci. 1 (1996) 96–100.
[15] J.G. Choi, J. Catal. 182 (1999) 104–116.
[16] X.W. Chen, T. Zhang, M.Y. Zheng, L.G. Xia, T. Li, W.C. Wu, X.D. Wang, C. Li, Ind. Eng. Chem. Res. 43 (2004) 6040–6047.
[17] M.J. Ledoux, P. DelGallo, C. PhamHuu, A.P.E. York, Catal. Today 27 (1996) 145–150.
[18] E. Furimsky, Appl. Catal. A 240 (2003) 1–28.
[19] Z.W. Chen, D. Higgins, A.P. Yu, L. Zhang, J.J. Zhang, Energ. Environ. Sci. 4 (2011) 3167–3192.
[20] C. Yang, H.B. Zhao, Y.L. Hou, D. Ma, J. Am. Chem. Soc. 134 (2012) 15814–15821.
[21] Y. Liu, T.G. Kelly, J.G.G. Chen, W.E. Mustain, ACS Catal. 3 (2013) 1184–1194.
[22] L.S. Zhong, F. Yu, Y.L. An, Y.H. Zhao, Y.H. Sun, Z.J. Li, T.J. Lin, Y.J. Lin, X.Z. Qi, Y.Y. Dai, L. Gu, J.S. Hu, S.F. Jin, Q. Shen, H. Wang, Nature 538 (2016) 84–87.
[23] Y. Ma, G. Guan, X. Hao, J. Cao, A. Abudula, Renew. Sustain. Energy Rev. 75 (2017) 1101–1129.
[24] L.L. Lin, W. Zhou, R. Gao, S.Y. Yao, X. Zhang, W.Q. Xu, S.J. Zheng, Z. Jiang, Q.L. Yu, Y.W. Li, C. Shi, X.D. Wen, D. Ma, Nature 544 (2017) 80–83.
[25] X. Zhang, C. Shi, B. Chen, A.N. Kuhn, D. Ma, H. Yang, Curr. Opin. Chem. Eng. 20 (2018) 68–77.
[26] S. Emin, C. Altinkaya, A. Semerci, H. Okuyucu, A. Yildiz, P. Stefanov, Appl. Catal. B 236 (2018) 147–153.
[27] A. Wang, T. Zhang, Acc. Chem. Res. 46 (2013) 1377–1386.
[28] C. Li, X. Zhao, A. Wang, G.W. Huber, T. Zhang, Chem. Rev. 115 (2015) 11559–11624.
[29] A.M. Robinson, J.E. Hensley, J.W. Medlin, ACS Catal. 6 (2016) 5026–5043.
[30] J.G. Chen, Chem. Rev. 96 (1996) 1477–1498.
[31] J. Pang, J. Li, Ceram. Int. 35 (2009) 3517–3520.
[32] V.P. Reva, V.Y. Yagofarov, A.E. Filatenkov, D.A. Gulevskii, V.G. Kuryavyi, Y.N. Mansurov, Refract. Ind. Ceram 58 (2017) 169–173.
[33] J.S. Lee, M.H. Yeom, K.Y. Park, I.-S. Nam, J.S. Chung, Y.G. Kim, S.H. Moon, J. Catal. 128 (1991) 126–136.
[34] T. Ishii, K. Yamada, N. Osuga, Y. Imashiro, J. Ozaki, ACS Omega 1 (2016) 689–695.
[35] A.M. Alexander, J.S.J. Hargreaves, Chem. Soc. Rev. 39 (2010) 4388–4401.
[36] C. Liang, P. Ying, C. Li, Chem. Mater. 14 (2002) 3148–3151.
[37] Y. Zhang, A. Wang, T. Zhang, Chem. Commun. 46 (2010) 862–864.
[38] J. Han, J. Duan, P. Chen, H. Lou, X. Zheng, H. Hong, Green Chem. 13 (2011) 2561–2568.
[39] A.T. Garcia-Esparza, D. Cha, Y. Ou, J. Kubota, K. Domen, K. Takanabe, ChemSusChem 6 (2013) 168–181.
[40] M. Chen, J. Zhang, Q. Chen, M. Qi, X. Xia, Mater. Res. Bull. 73 (2016) 459–464.
[41] H.Y. Wang, S.D. Liu, B. Liu, V. Montes, J.M. Hill, K.J. Smith, J. Solid State Chem. 258 (2018) 818–824.
[42] C. Giordano, C. Erpen, W. Yao, M. Antonietti, Nano Lett. 8 (2008) 4659–4663.
[43] C. Giordano, M. Antonietti, Nano Today 6 (2011) 366–380.
[44] X. Liu, C. Kunkel, P. Ramírez de la Piscina, N. Homs, F. Viñes, F. Illas, ACS Catal. 7 (2017) 4323–4335.
[45] C. Wan, N.A. Knight, B.M. Leonard, Chem. Commun. 49 (2013) 10409–10411.
[46] H. Wang, A. Wang, X. Wang, T. Zhang, Chem. Commun. (2008) 2565–2567.
[47] C. Wan, Y.N. Regmi, B.M. Leonard, Angew. Chem. Int. Ed. 126 (2014) 6525–6528.
[48] Y. Gu, Z. Li, L. Chen, Y. Ying, Y. Qian, Mater. Res. Bull. 38 (2003) 1119–1122.
[49] F.G. Baddour, C.P. Nash, J.A. Schaidle, D.A. Ruddy, Angew. Chem. Int. Ed. 55 (2016) 9026–9029.
[50] L. Han, M. Xu, Y. Han, Y. Yu, S. Dong, ChemSusChem 9 (2016) 2784–2787.
[51] Y. Xu, X. Xiao, Z. Ye, S. Zhao, R. Shen, C. He, J. Zhang, Y. Li, X. Chen, J. Am. Chem. Soc. 139 (2017) 5285–5288.
[52] J. Wan, J.B. Wu, X. Gao, T.Q. Li, Z.M. Hu, H.M. Yu, L. Huang, Adv. Funct. Mater. 27 (2017).
[53] H. Yu, H. Fan, J. Wang, Y. Zheng, Z. Dai, Y. Lu, J. Kong, X. Wang, Y.J. Kim, Q. Yan, J.-M. Lee, Nanoscale 9 (2017) 7260–7267.
[54] J. Zhu, K. Sakaushi, G. Clavel, M. Shalom, M. Antonietti, T.-P. Fellinger, J. Am. Chem. Soc. 137 (2015) 5480–5485.
[55] J. Chen, Y. Huang, F. Zhao, H. Ye, Y. Wang, J. Zhou, Y. Liu, Y. Li, J. Mater. Chem. A 5 (2017) 8125–8132.
[56] J.S. Lee, S.T. Oyama, M. Boudart, J. Catal. 106 (1987) 125–133.
[57] J.S. Lee, L. Volpe, F.H. Ribeiro, M. Boudart, J. Catal. 112 (1988) 44–53.
[58] J.B. Claridge, A.P.E. York, A.J. Brungs, M.L.H. Green, Chem. Mater. 12 (2000) 132–142.
[59] S.T. Hunt, T. Nimmanwudipong, Y. Román-Leshkov, Angew. Chem. Int. Ed. 53 (2014) 5131–5136.
[60] J. Jia, W. Zhou, Z. Wei, T. Xiong, G. Li, L. Zhao, X. Zhang, H. Liu, J. Zhou, S. Chen, Nano Energy 41 (2017) 749–757.
[61] B. Ren, D. Li, Q. Jin, H. Cui, C. Wang, J. Mater. Chem. A 5 (2017) 13196–13203.
[62] E.I. Ko, R.J. Madix, Surf. Sci. Lett. 100 (1980) L449–L453.
[63] H. Ren, Y. Chen, Y. Huang, W. Deng, D.G. Vlachos, J.G. Chen, Green Chem. 16 (2014) 761–769.
[64] J.M. Muller, G. F. G, Bull. Soc. Chim. France 2 (1970) 416.
[65] B.M. Tackett, W. Sheng, J.G. Chen, Joule 1 (2017) 253–263.
[66] E. Furimsky, Appl. Catal. A Gen. 240 (2003) 1–28.
[67] H.T. Luk, C. Mondelli, D.C. Ferre, J.A. Stewart, J. Perez-Ramirez, Chem. Soc. Rev. 46 (2017) 1358–1426.
[68] M.M. Sullivan, C.J. Chen, A. Bhan, Catal. Sci. Technol. 6 (2016) 602–616.
[69] S. Boullosa-Eiras, R. Lodeng, H. Bergem, M. Stocker, L. Hannevold, E.A. Blekkan, J.J. Spivey, Y.F. Han, K.M. Dooley (Eds.), Catalysis, 2014, pp. 29–71.
[70] C.E. Chan-Thaw, A. Villa, Appl. Sci.-Basel 8 (2018).
[71] B.C. Saha, J. Ind. Microbiol. Biotechnol. 30 (2003) 279–291.
[72] J. Pang, A. Wang, M. Zheng, T. Zhang, Chem. Commun. 46 (2010) 6935–6937.
[73] L. Hu, L. Lin, Z. Wu, S. Zhou, S. Liu, Appl. Catal. B 174-175 (2015) 225–243.
[74] J. Pang, A. Wang, M. Zheng, Y. Zhang, Y. Huang, X. Chen, T. Zhang, Green Chem. 14 (2012) 614–617.
[75] H. Kobayashi, A. Fukuoka, Green Chem. 15 (2013) 1740–1763.
[76] M. Yabushita, H. Kobayashi, A. Fukuoka, Appl. Catal. B 145 (2014) 1–9..
[77] A.M. Ruppert, K. Weinberg, R. Palkovits, Angew. Chem., Int. Ed. 51 (2012) 2564–2601.
[78] L. Negahdar, P.J.C. Hausoul, S. Palkovits, R. Palkovits, Appl. Catal. B 166-167 (2015) 460–464.
[79] N. Ji, T. Zhang, M. Zheng, A. Wang, H. Wang, X. Wang, J.G. Chen, Angew. Chem. Int. Ed. 47 (2008) 8510–8513.
[80] N. Ji, T. Zhang, M. Zheng, A. Wang, H. Wang, X. Wang, Y. Shu, A.L. Stottlemyer, J.G. Chen, Catal. Today 147 (2009) 77–85.
[81] J. Pang, M. Zheng, R. Sun, A. Wang, X. Wang, T. Zhang, Green Chem. 18 (2016) 342–359.
[82] M. Zheng, J. Pang, R. Sun, A. Wang, T. Zhang, ACS Catal. 7 (2017) 1939–1954.
[83] P.S. Shuttleworth, M. De bruyn, H.L. Parker, A.J. Hunt, V.L. Budarin, A.S. Matharu, J.H. Clark, Green Chem. 16 (2014) 573–584.
[84] J. Pang, M. Zheng, X. Li, Y. Jiang, Y. Zhao, A. Wang, J. Wang, X. Wang, T. Zhang, Appl. Catal. B 239 (2018) 300–308.
[85] N. Ji, M. Zheng, A. Wang, T. Zhang, J.G. Chen, ChemSusChem 5 (2012) 939–944.
[86] C.B. Rodella, D.H. Barrett, S.F. Moya, S.J.A. Figueroa, M.T.B. Pimenta, A.A.S. Curvelo, V. Teixeira da Silva, RSC Adv. 5 (2015) 23874–23885.
[87] G.F. Leal, S.F. Moya, D.M. Meira, D.H. Barrett, E. Teixeira-Neto, A.A.S. Curvelo, V. Teixeira da Silva, C.B. Rodella, RSC Adv. 6 (2016) 87756–87766.
[88] W.M. Wan, B.M. Tackett, J.G.G. Chen, Chem. Soc. Rev. 46 (2017) 1807–1823.
[89] R. Ooms, M. Dusselier, J.A. Geboers, B. Op de Beeck, R. Verhaeven, E. Gobechiya, J.A. Martens, A. Redl, B.F. Sels, Green Chem. 16 (2014) 695–707.
[90] L. Zhou, A. Wang, C. Li, M. Zheng, T. Zhang, ChemSusChem 5 (2012) 932–938.
[91] J. Pang, M. Zheng, A. Wang, T. Zhang, Ind. Eng. Chem. Res. 50 (2011) 6601–6608.
[92] J. Pang, M. Zheng, A. Wang, R. Sun, H. Wang, Y. Jiang, T. Zhang, AlChE J. 60 (2014) 2254–2262.
[93] K. Fabicovicova, M. Lucas, P. Claus, Green Chem. 17 (2015) 3075–3083.
[94] K. Fabicovicova, M. Lucas, P. Claus, ChemSusChem 9 (2016) 2804–2815.
[95] Z. Tai, J. Zhang, A. Wang, M. Zheng, T. Zhang, Chem. Commun. 48 (2012) 7052–7054.
[96] Z. Tai, J. Zhang, A. Wang, J. Pang, M. Zheng, T. Zhang, ChemSusChem 6 (2013) 652–658.
[97] T.D.H. Bugg, R. Rahmanpour, Curr. Opin. Chem. Biol. 29 (2015) 10–17.
[98] J. Zakzeski, P.C.A. Bruijnincx, A.L. Jongerius, B.M. Weckhuysen, Chem. Rev. 110 (2010) 3552–3599.
[99] C. Xu, R.A.D. Arancon, J. Labidi, R. Luque, Chem. Soc. Rev. 43 (2014) 7485–7500.
[100] H.L. Wang, H.M. Wang, E. Kuhn, M.P. Tucker, B. Yang, ChemSusChem 11 (2018) 285–291.
[101] A. Agarwal, M. Rana, J.-H. Park, Fuel Process. Technol. 181 (2018) 115–132.
[102] J. Sun, A.M. Karim, X.S. Li, J. Rainbolt, L. Kovarik, Y. Shin, Y. Wang, Chem. Commun. 51 (2015) 16617–16620.

[103] Y.T. Cheng, Z. Wang, C.J. Gilbert, W. Fan, G.W. Huber, Angew. Chem. Int. Ed. 51 (2012) 11097–11100.
[104] B.M. Upton, A.M. Kasko, Chem. Rev. 116 (2016) 2275–2306.
[105] C. Li, M. Zheng, A. Wang, T. Zhang, Energy Environ. Sci. 5 (2012) 6383–6390.
[106] H. Guo, B. Zhang, C. Li, C. Peng, T. Dai, H. Xie, A. Wang, T. Zhang, ChemSusChem 9 (2016) 3220–3229.
[107] H. Guo, B. Zhang, Z. Qi, C. Li, J. Ji, T. Dai, A. Wang, T. Zhang, ChemSusChem 10 (2017) 523–532.
[108] R. Ma, W. Hao, X. Ma, Y. Tian, Y. Li, Angew. Chem. Int. Ed. 53 (2014) 7310–7315.
[109] X. Ma, R. Ma, W. Hao, M. Chen, F. Yan, K. Cui, Y. Tian, Y. Li, ACS Catal. 5 (2015) 4803–4813.
[110] F. Yan, R. Ma, X. Ma, K. Cui, K. Wu, M. Chen, Y. Li, Appl. Catal. B 202 (2017) 305–313.
[111] R. Ma, K. Cui, L. Yang, X. Ma, Y. Li, Chem. Commun. 51 (2015) 10299–10301.
[112] W. Schutyser, G. Van den Bossche, A. Raaffels, S. Van den Bosch, S.F. Koelewijn, T. Renders, B.F. Sels, ACS Sustain. Chem. Eng. 4 (2016) 5336–5346.
[113] L. Cattelan, A.K.L. Yuen, M.Y. Lui, A.F. Masters, M. Selva, A. Perosa, T. Maschmeyer, ChemCatChem 9 (2017) 2717–2726.
[114] X. Yang, M. Feng, J.-S. Choi, H.M. Meyer, B. Yang, Fuel 244 (2019) 528–535.
[115] R. De Clercq, M. Dusselier, B.F. Sels, Green Chem. 19 (2017) 5012–5040.
[116] M. Asadieraghi, W.M.A. Wan Daud, H.F. Abbas, Renew. Sustain. Energy Rev. 36 (2014) 286–303.
[117] H. Wang, M. Feng, B. Yang, Green Chem. 19 (2017) 1668–1673.
[118] X. Zhang, H. Lei, S. Chen, J. Wu, Green Chem. 18 (2016) 4145–4169.
[119] Q. Han, M.U. Rehman, J. Wang, A. Rykov, O.Y. Gutiérrez, Y. Zhao, S. Wang, X. Ma, J.A. Lercher, Appl. Catal. B 253 (2019) 348–358.
[120] J. Han, J. Duan, P. Chen, H. Lou, X. Zheng, Adv. Synth. Catal. 353 (2011) 2577–2583.
[121] J. Han, J. Duan, P. Chen, H. Lou, X. Zheng, H. Hong, ChemSusChem 5 (2012) 727–733.
[122] F. Wang, J. Jiang, K. Wang, Q. Zhai, F. Long, P. Liu, J. Feng, H. Xia, J. Ye, J. Li, J. Xu, Appl. Catal. B 242 (2019) 150–160.
[123] R.W. Gosselink, D.R. Stellwagen, J.H. Bitter, Angew. Chem. Int. Ed. 52 (2013) 5089–5092.
[124] P.M. Mortensen, H.W.P. de Carvalho, J.D. Grunwaldt, P.A. Jensen, A.D. Jensen, J. Catal. 328 (2015) 208–215.
[125] F. Wang, J. Xu, J. Jiang, P. Liu, F. Li, J. Ye, M. Zhou, Fuel 216 (2018) 738–746.
[126] S.K. Kim, D. Yoon, S.C. Lee, J. Kim, ACS Catal. 5 (2015) 3292–3303.
[127] D.R. Stellwagen, J.H. Bitter, Green Chem. 17 (2015) 582–593.
[128] L. Souza Macedo, R.R. Oliveira, T. van Haasterecht, V. Teixeira da Silva, H. Bitter, Appl. Catal. B 241 (2019) 81–88.
[129] H. Wang, S. Yan, S.O. Salley, K.Y. Simon Ng, Fuel 111 (2013) 81–87.
[130] J.A. Schaidle, J. Blackburn, C.A. Farberow, C. Nash, K.X. Steirer, J. Clark, D.J. Robichaud, D.A. Ruddy, ACS Catal. 6 (2016) 1181–1197.
[131] M.M. Sullivan, A. Bhan, ACS Catal. 6 (2016) 1145–1152.
[132] A.L. Jongerius, R.W. Gosselink, J. Dijkstra, J.H. Bitter, P.C.A. Bruijnincx, B.M. Weckhuysen, ChemCatChem 5 (2013) 2964–2972.
[133] A.L. Jongerius, P.C.A. Bruijnincx, B.M. Weckhuysen, Green Chem. 15 (2013) 3049–3056.
[134] Y.X. Chen, Y. Zheng, M. Li, X.F. Zhu, Fuel Process. Technol. 134 (2015) 46–51.
[135] M.A. Machado, S. He, T.E. Davies, K. Seshan, V. Teixeira da Silva, Catal. Today 302 (2018) 161–168.
[136] Q. Lu, M. Zhou, W. Li, X. Wang, M. Cui, Y. Yang, Catal. Today 302 (2018) 169–179.
[137] J. Engelhardt, P.B. Lyu, P. Nachtigall, F. Schuth, A.M. Garcia, ChemCatChem 9 (2017) 1985–1991.
[138] H. Fang, J. Du, C. Tian, J. Zheng, X. Duan, L. Ye, Y. Yuan, Chem. Commun. 53 (2017) 10295–10298.
[139] E. Ochoa, D. Torres, R. Moreira, J.L. Pinilla, I. Suelves, Appl. Catal. B 239 (2018) 463–474.
[140] S. Boullosa-Eiras, R. Lødeng, H. Bergem, M. Stöcker, L. Hannevold, E.A. Blekkan, Catal. Today 223 (2014) 44–53.
[141] W.S. Lee, Z. Wang, R.J. Wu, A. Bhan, J. Catal. 319 (2014) 44–53.
[142] T. Iida, M. Shetty, K. Murugappan, Z. Wang, K. Ohara, T. Wakihara, Y. Román-Leshkov, ACS Catal. 7 (2017) 8147–8151.
[143] S. Liu, H. Wang, K.J. Smith, C.S. Kim, Energ. Fuel 31 (2017) 6378–6388.
[144] R. Liu, M. Pang, X. Chen, C. Li, C. Xu, C. Liang, Catal. Sci. Technol. 7 (2017) 1333–1341.
[145] R. Moreira, E. Ochoa, J.L. Pinilla, A. Portugal, I. Suelves, Catalysts 8 (2018) 127.
[146] W.-S. Lee, Z. Wang, W. Zheng, D.G. Vlachos, A. Bhan, Catal. Sci. Technol. 4 (2014) 2340–2352.
[147] Z. Lin, R. Chen, Z. Qu, J.G. Chen, Green Chem. 20 (2018) 2679–2696.
[148] H. Fang, A. Roldan, C. Tian, Y. Zheng, X. Duan, K. Chen, L. Ye, S. Leoni, Y. Yuan, J. Catal. 369 (2019) 283–295.
[149] A.L. Stottlemyer, T.G. Kelly, Q. Meng, J.G. Chen, Surf. Sci. Rep. 67 (2012) 201–232.
[150] H. Ren, W. Yu, M. Salciccioli, Y. Chen, Y. Huang, K. Xiong, D.G. Vlachos, J.G. Chen, ChemSusChem 6 (2013) 798–801.
[151] T.G. Kelly, J.G. Chen, Green Chem. 16 (2014) 777–784.
[152] K. Xiong, W.S. Lee, A. Bhan, J.G. Chen, ChemSusChem 7 (2014) 2146–2149.
[153] W. Wan, Z. Jiang, J.G. Chen, Top. Catal. 61 (2018) 439–445.
[154] Z. Lin, W. Wan, S. Yao, J.G. Chen, Appl. Catal. B 233 (2018) 160–166.
[155] Y. Shi, Y. Yang, Y.W. Li, H. Jiao, ACS Catal. 6 (2016) 6790–6803.
[156] J.R. McManus, J.M. Vohs, Surf. Sci. 630 (2014) 16–21.
[157] Y. Deng, R. Gao, L. Lin, T. Liu, X.-D. Wen, S. Wang, D. Ma, J. Am. Chem. Soc. 140 (2018) 14481–14489.
[158] G. Li, N. Li, J. Yang, A. Wang, X. Wang, Y. Cong, T. Zhang, Bioresour. Technol. 134 (2013) 66–72.
[159] J. Rogowski, M. Andrzejczuk, J. Berlowska, M. Binczarski, D. Kregiel, A. Kubiak, M. Modelska, E. Szubiakiewicz, A. Stanishevsky, J. Tomaszewska, I.A. Witonska, Molecules 22 (2017) 2033.
[160] Y.B. Huang, M.Y. Chen, L. Yan, Q.X. Guo, Y. Fu, ChemSusChem 7 (2014) 1068–1072.
[161] M. Braun, M. Antonietti, Green Chem. 19 (2017) 3813–3819.
[162] D.M. Alonso, S.G. Wettstein, J.A. Dumesic, Green Chem. 15 (2013) 584–595.
[163] K. Yan, Y. Yang, J. Chai, Y. Lu, Appl. Catal. B 179 (2015) 292–304.
[164] E.F. Mai, M.A. Machado, T.E. Davies, J.A. Lopez-Sanchez, V. Teixeira da Silva, Green Chem. 16 (2014) 4092–4097.
[165] J. Quiroz, E.F. Mai, V.T. da Silva, Top. Catal. 59 (2016) 148–158.
[166] T. Dai, C. Li, L. Li, Z.K. Zhao, B. Zhang, Y. Cong, A. Wang, Angew. Chem. Int. Ed. 57 (2018) 1808–1812.
[167] M.M. Moyer, C. Karakaya, R.J. Kee, B.G. Trewyn, ChemCatChem 9 (2017) 3090–3101.
[168] S.T. Hunt, T. Nimmanwudipong, Y. Roman-Leshkov, Angew. Chem. Int. Ed. 53 (2014) 5131–5136.
[169] H.H. Hwu, J.G. Chen, Chem. Rev. 105 (2005) 185–212.
[170] T. He, X.X. Liu, Y.Z. Ge, D.Z. Han, J.Q. Li, Z.Q. Wang, J.H. Wu, Catal. Commun. 102 (2017) 127–130.
[171] C. Wang, W.L. Gu, J.H. Li, D.Y. Huang, W.P. Lu, Y. Huang, M. Wu, Energy Technol. 5 (2017) 2216–2225.
[172] S. Boullosa-Eiras, R. Lodeng, H. Bergem, M. Stocker, L. Hannevold, E.A. Blekkan, J.J. Spivey, Y.F. Han, K.M. Dooley (Eds.), Catalysis, Vol. 26 2014, pp. 29–71.
[173] L. Souza Macedo, D.R. Stellwagen, V. Teixeira da Silva, J.H. Bitter, ChemCatChem 7 (2015) 2816–2823.
[174] C.J. Chen, A. Bhan, ACS Catal. 7 (2017) 1113–1122.
[175] F.G. Baddour, V.A. Witte, C.P. Nash, M.B. Griffin, D.A. Ruddy, J.A. Schaidle, ACS Sustain. Chem. Eng. 5 (2017) 11433–11439.
[176] M. Zhou, L. Cheng, J.S. Choi, B. Liu, L.A. Curtiss, R.S. Assary, J. Phys. Chem. C 122 (2018) 1595–1603.
[177] Y. Shi, Y. Yang, Y.W. Li, H. Jiao, Appl. Catal. A Gen. 524 (2016) 223–236.
[178] Q. Bkour, O.G. Marin-Flores, M.G. Norton, S. Ha, Appl. Catal. B 245 (2019) 613–622.
[179] L. Wei, R. Bibi, Y. Zheng, W. Tian, L. Chen, N. Li, J. Zhou, Catal. Lett. 148 (2018) 1856–1869.
[180] J.H. Chen, F.M. Zhai, M. Liu, X.M. Hou, K.C. Chou, Langmuir 32 (2016) 5909–5916.
[181] L. Wang, S. Zhu, N. Marinkovic, S. Kattel, M. Shao, B. Yang, J.G. Chen, Appl. Catal. B 232 (2018) 365–370.
[182] Y.-J. Ko, J.-M. Cho, I. Kim, D.S. Jeong, K.-S. Lee, J.-K. Park, Y.-J. Baik, H.-J. Choi, W.-S. Lee, Appl. Catal. B 203 (2017) 684–691.
[183] M.G. Granados-Fitch, J.M. Quintana-Melgoza, E.A. Juarez-Arellano, M. Avalos-Borja, Int. J. Hydrog. Energy 44 (2019) 2784–2796.
[184] X. Zhang, Z. Zhang, Z. Zhou, J. Engery Chem. 27 (2018) 73–85.
[185] J. Pang, R.G. Mendes, A. Bachmatiuk, L. Zhao, H.Q. Ta, T. Gemming, H. Liu, Z. Liu, M.H. Rummeli, Chem. Soc. Rev. 48 (2019) 72–133.
[186] S.Y. Yao, X. Zhang, W. Zhou, R. Gao, W.Q. Xu, Y.F. Ye, L.L. Lin, X.D. Wen, P. Liu, B.B. Chen, E. Crumlin, J.H. Guo, Z.J. Zuo, W.Z. Li, J.L. Xie, L. Lu, C.J. Kiely, L. Gu, C. Shi, J.A. Rodriguez, D. Ma, Science 357 (2017) 389–392.
[187] J. Zakzeski, R.J.H. Grisel, A.T. Smit, B.M. Weckhuysen, ChemSusChem 5 (2012) 430–437.
[188] N.S. Gould, B. Xu, Chem. Sci. 9 (2018) 281–287.
[189] H. Wang, Prog. Surf. Sci. 91 (2016) 155–182.
[190] K. Murugappan, E.M. Anderson, D. Teschner, T.E. Jones, K. Skorupska, Y. Román-Leshkov, Nat. Catal. 1 (2018) 960–967.